8260 J. Med. Chem. 2010, 53, 8260–8273
DOI: 10.1021/jm1004545

Journal of Medicinal Chemistry Article

Synthesis and Identification of New 4-Arylidene Curcumin Analogues as Potential Anticancer Agents Targeting Nuclear Factor-κB Signaling Pathway

Xu Qiu,[†,§] Yuhong Du,[‡,§] Bin Lou,[‡] Yinglin Zuo,[†] Weiyan Shao,[†] Yingpeng Huo,[†] Jianing Huang,[†] Yanjun Yu,[†] Binhua Zhou,[†] Jun Du,[†] Haian Fu,*[,‡] and Xianzhang Bu*[,†]

[†]*School of Pharmaceutical Sciences, Sun Yat-sen University, Guangzhou 510275, China, and* [‡]*Department of Pharmacology and Emory Chemical Biology Discovery Center, Emory University School of Medicine, 1510 Clifton Road, Atlanta, Georgia 30322, United States.* [§] *These authors contributed equally to this work.*

Received April 13, 2010

A series of curcumin analogues including new 4-arylidene curcumin analogues (4-arylidene-1,7-bisarylhepta-1,6-diene-3,5-diones) were synthesized. Cell growth inhibition assays revealed that most 4-arylidene curcumin analogues can effectively decrease the growth of a panel of lung cancer cells at submicromolar and low micromolar concentrations. High content analysis technology coupled with biochemical studies showed that this new class of 4-arylidene curcumin analogues exhibits significantly improved NF-κB inhibition activity over the parent compound curcumin, at least in part by inhibiting IκB phosphorylation and degradation via IKK blockage; selected 4-arylidene curcumin analogues also reduced the tumorigenic potential of cancer cells in a clonogenic assay.

Introduction

Nuclear factor-κB (NF-κB[a]) proteins are a family of structurally related eukaryotic transcription factors with a conserved reticuloendotheliosis (Rel) domain.[1] They influence gene expression events that impact a large number of physiological processes including immune response, cell survival, differentiation, and proliferation.[2] Before cell stimulation, NF-κB dimers are inactive in the cytoplasm and mainly regulated by two distinct signaling pathways.[3] The canonical NF-κB activation pathway has been extensively studied. Prior to activation, NF-κB dimers composed of RelA (also known as p65), c-REL, and p50 are retained in the cytoplasm by inhibitory κB (IκB) proteins. Various extracellular signals, such as those from microbial infections, viral infections, and proinflammatory cytokines, activate the IκB kinase (IKK) complex. The IKK complex targets NF-κB-bound IκBs by phosphorylating two conserved serine residues, which drives ubiquitin-mediated degradation of IκB and leads to the liberation and subsequent nuclear translocation of released NF-κB dimers. Phosphorylation of IκB mainly depends on the IKKβ catalytic subunit of the IKK complex in the canonical pathway. In the second pathway of NF-κB activation, NF-κB, typically exists as an RelB/p100 dimer and remains inactivated by p100 instead of IκB. After stimulation by certain signals, such as the tumor-necrosis factor (TNF) cytokine family member lymphotoxin B (LTβ), an IKKα homodimer, along with NF-κB inducing kinase (NIK), induces the phosphorylation and proteasome-mediated processing of p100 to generate p52, resulting in the production of an active p52/RelB dimer and its translocation to the nucleus.

Recent advances have revealed key roles of NF-κB signaling in pathological conditions such as oncogenesis and inflammation. NF-κB is commonly overexpressed and constitutively activated in different types of hematologic cancers and solid tumors.[4−7] Constitutive activation of NF-κB promotes tumor proliferation, invasion, and metastasis;[8,9] moreover, NF-κB activation allows malignant cells to escape apoptosis and therefore contributes to radiation and chemotherapy resistance in cancer cells.[10−12] Noticeably, many chemotherapeutic agents have been found to activate NF-κB via various approaches, leading to chemoresistance and subsequent failure of chemotherapy.[13,14] Accumulating evidence suggests that inhibition of NF-κB activation can prevent tumor resistance to chemotherapeutic agents, shift the death−survival balance toward apoptosis, and improve the efficacy of current chemotherapeutic regimens.[15,16]

A large number of compounds have been reported to inhibit NF-κB by interacting with key macromolecules in the signaling pathway. Many natural dietary agents, such as soya isoflavone,[17] resveratrol,[18] and curcumin,[19] have been found to inhibit NF-κB and induce apoptosis in tumor cells. Curcumin (diferuloylmethane), a yellow spice and pigment isolated from the rhizome of *Curcuma longa*, has been used as a spice in South Asia for centuries. It has attracted much attention because of its broad range of bioactivities,[20] including antioxidative, anti-inflammatory, and anticancer activities, as well as its pharmacological safety and potency as chemopreventive agent.[21] One of the predominant targets of curcumin is the NF-κB cell signaling pathway.[22] Curcumin directly inhibits IKK and the 26S proteasome[23,24] to block NF-κB activation. Unfortunately, the clinical potential of curcumin remains limited because of its relatively low potency and poor

*To whom correspondence should be addressed. For H.F.: phone, 404-727-0365; fax, 404-727-0365; e-mail: hfu@emory.edu. For X.B.: phone and fax, 020-39942054; e-mail, phsbxzh@mail.sysu.edu.cn.

[a] Abbreviations: NF-κB, nuclear factor-κB; Rel, reticuloendotheliosis; IκB, inhibitor of κB; IKK, inhibitor of κB kinase; NIK, NF-κB inducing kinase; TNF, tumor-necrosis factor; LTβ, lymphotoxin B; GST, glutathione *S*-transferase; TCA, trichloroacetic acid; SRB, sulforhodamine B.

 Published on Web 11/11/2010 © 2010 American Chemical Society

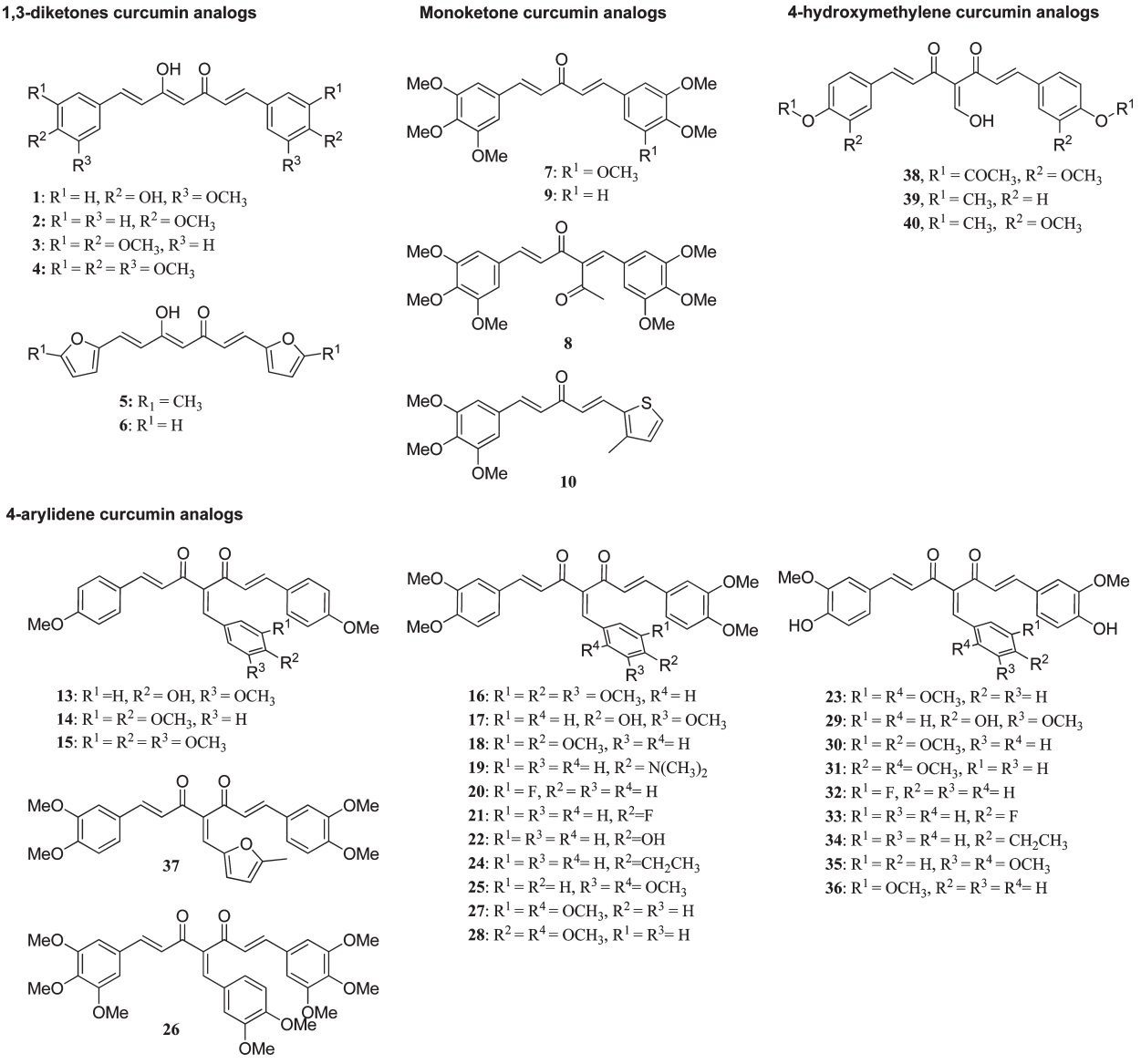

Figure 1. Structures of 1,3-diketones curcumin analogues (**1**−**6**), monoketone curcumin analogues (**7**−**10**), 4-arylidene crucumin analogues (**13**−**37**), and 4-hydroxymethylene curcumin analogues (**38**−**40**).

bioavailability.[25] Attempts have been made by others to chemically modify curcumin in order to increase its activity against cancer and NF-κB.[26−31] However, most of these investigations have focused on design, synthesis, and activity of 1,3-diketones and monoketone analogues of curcumin. However, curcuminoids, such as Knoevenagel condensates of curcumin analogues, contain a novel skeleton and remain quite less investigated.[28,32,33] In 2006, Ajit P. Zambre et al. reported that copper(II) conjugates of Knoevenagel condensates of curcumin showed potential in inhibiting TNFα induced NF-κB activation.[28] Nevertheless, highly active and clinically promising curcuminoids remain to be developed. A systematic investigation of current curcumin analogues would greatly facilitate the development of new curcumin analogues for therapeutic interventions. In the present study, we describe the synthesis and identification of new 4-arylidene curcumin analogues (Knoevenagel condensates of 1,3-diketones curcumin analogues with aromatic aldehydes) as a new class of potential anticancer agents. Screening of the synthesized compounds with high content analysis technology, coupled with biochemical studies, revealed that 4-arylidene curcumin analogues have significantly improved IKK/NF-κB inhibition activity and elevated cytotoxicity over the parent compound curcumin. These compounds effectively decreased growth and reduced the tumorigenic potential of cancer cells, as seen in a clonogenic assay.

Results and Discussion

Chemistry. To search for potent analogues with favorable medicinal properties, we extended the molecular diversity of curcuminiods by designing three types of curcuminoids: 1,3-diketones curcumin analogues, monoketone curcumin analogues, and 4-arylidene curcumin analogues (4-arylidene-1, 7-bisarylhepta-1,6-diene-3,5-diones) (Figure 1).

Classical 1,3-diketones (**1**−**6**) including curcumin (**1**) and a representative 1,3-diketone derivative with known activity (**3**)[34] were synthesized using a previously reported procedure[35] with slight modification (Scheme 1). Briefly, to protect the C-3 of acetylacetone from an unwanted Knoevenagel reaction, a boric acetylacetone anhydride complex was prepared first by refluxing acetylacetone with boric anhydride in EtOAc. The final products **1**−**6** were synthesized by aldol

condensation of protected acetylacetone aromatic aldehydes as described.

Monoketone curcumin analogues have been extensively investigated because of their potential anticancer activities. **7** has been reported to have high activity in antitumor assays[36] and was therefore considered; **9** and **10** are asymmetric analogues of **7**. These three compounds were included in our work to represent monoketone curcumin analogues. **7** and the intermediate **11** were synthesized by treating 3,4,5-trimethoxybenzaldehyde with excess acetone in the presence of KOH. **9** and **10** were synthesized by condensing **11** with veratraldehyde and 3-methylthiophene-2-carbaldehyde, respectively. Furthermore, another new compound, **8**, was prepared by condensing **12** and 3,4,5-trimethoxybenzaldehyde. The intermediate **12** was obtained using the same conditions as in the synthesis of **1**−**6** except the excess protected acetylacetone (Scheme 2).

Compared to the large number of traditional 1,3-diketones and monoketone curcumin analogues that have been designed and evaluated, investigation of Knoevenagel condensates of curcuminoids remains scarce. In our current work, 23 new 4-arylidene curcumin analogues (Knoevenagel condensates **13**−**17**, **19**−**28**, **30**−**37**) were designed and synthesized by coupling **1**−**4** with different aromatic aldehydes in toluene with AcOH and piperidine as a catalyst. The known 4-arylidene curcumin analogues **18** and **29** were synthesized under the same conditions except with acetylacetone and aldehydes as reactants (Scheme 1).

The 4-arylidene modification can induce a change of a partial enolic diketone, which is universal in 1,3-diketones curcumin analogues, to an absolute diketone moiety, possibly affecting bioactivity. To explore the effect of this transition, three new 4-hydroxymethylene curcumin analogues (**38**−**40**, Figure 1), which possess absolute diketone moieties, were designed as references. **38**, **39**, and **40** were synthesized by refluxing triethoxymethane and Ac_2O with **1**, **2**, and **3**, respectively (Scheme 3).

New 4-Arylidene Crucumin Analogues Exhibit Potent Inhibitory Activity against Caner Cells. In order to evaluate the anticancer activities of new curcumin derivatives, we tested the effects of synthesized compounds on the growth of A549 lung adenocarcinoma cells. For comparison, dose-response experiments were carried out to obtain GI_{50} values for each compound as previously described,[37] with curcumin (**1**) as a control. As summarized in Table 1, all the traditional 1,3-diketone cucumin analogues (**1**−**6**) showed moderate to poor activity against A549 growth, while improved antiproliferation activities of monoketone analogues **7** and **9** were observed (GI_{50} of 0.53 and 1.21 μM respectively).

At the same time, the thiophene ring moiety bearing **10** (GI_{50} = 9.31 μM) showed decreased activity compared to **7** and **9**, indicating that S replacement of the O atom in the heterocycle of **9** made a negative contribution to its activity. As a regioisomer of **4**, the Knoevenagel condensate **8** exhibited much higher activity (GI_{50} = 0.53 μM) than **4**. **8** can also be regarded as a monoketone curumin analogue with an acetyl substitution. When the activities of **7**−**9** and **1**−**6** were compared, it was revealed that the spacing of the two aromatic rings most likely influences the activity of curcumin analogues against A549 growth. The close activities of **8** and **7** indicated that the acetyl group has no apparent effect on activity against A549 growth.

Remarkably, most of the 4-arylidene curcumin analogues (4-arylidene-1,7-bisarylhepta-1,6-diene-3, 5-diones, **13**−**37**) showed potent anticancer activities with a GI_{50} in the submicromolar range (0.23−0.93 μM), except **15**, **19**, **29**, and **37** which exhibited slightly lower activities (GI_{50} of 1.12−2.62 μM). The potency of 4-arylidene analogues was improved by 10- to 60-fold over the parent compound curcumin in this assay. 4-Hydroxymethylene curcumin analogues (**38**−**40**), however, showed poor activity, suggesting the importance of

Scheme 1. Synthesis of Compounds **1**−**6** and **13**−**37**[a]

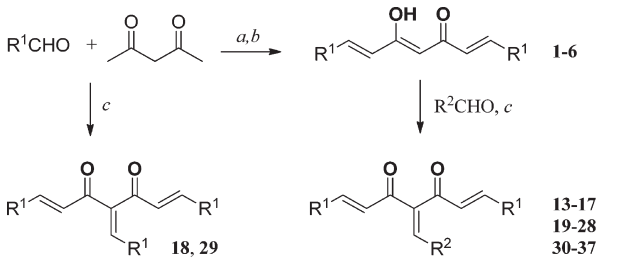

[a] Reagents and conditions: (a) B_2O_3, B(*n*-BuO)$_3$, *n*-$BuNH_2$; (b) HCl; (c) piperidine, AcOH, toluene, 140 °C.

Scheme 3. Synthesis of Compounds **38**−**40**[a]

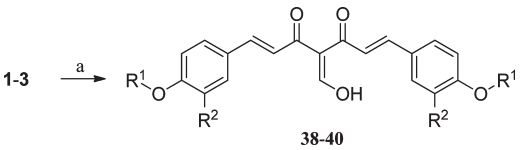

[a] Reagents and conditions: (a) triethoxymethane, Ac_2O, 140 °C, 5 h.

Scheme 2. Synthesis of Compounds **7**−**10**[a]

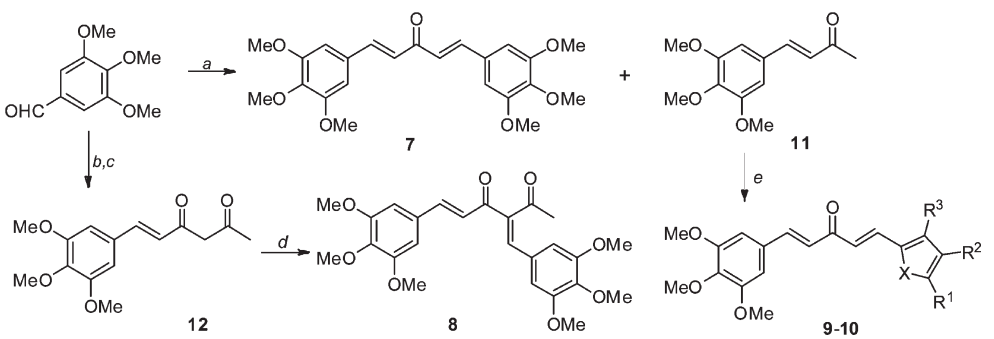

[a] Reagents and conditions: (a) excess acetone, KOH/H_2O, MeOH; (b) pre-mixed acetylacetone and B(*n*-BuO)$_3$, *n*-$BuNH_2$, 80 °C to room temperature; (c) HCl, room temperature; (d) 3,4,5-trimethoxybenzaldehyde, DMF, reflux; (e) veratraldehyde or 3-methylthiophene-2-carbaldehyde, KOH/H_2O, MeOH.

Table 1. Effect of Curcumin and Its Analogues on Growth of A549 Cells[a]

Growth Inhibition of A549 Cells					
compd	GI_{50} (μM)	compd	GI_{50} (μM)	compd	GI_{50} (μM)
curcumin	15.23	**16**	0.23	**29**	2.00
2	>25	**17**	0.53	**30**	0.43
3	5.80	**18**	0.31	**31**	0.69
4	19.26	**19**	2.62	**32**	0.36
5	>25	**20**	0.58	**33**	0.78
6	>25	**21**	0.55	**34**	0.55
7	0.55	**22**	0.42	**35**	0.42
8	0.53	**23**	0.67	**36**	0.64
9	1.21	**24**	0.63	**37**	1.31
10	9.31	**25**	0.67	**38**	>25
13	1.64	**26**	0.37	**39**	>25
14	0.93	**27**	0.53	**40**	>25
15	1.12	**28**	0.65		

[a] Human adenocarcinoma A549 cells were seeded for 12 h, subsequently incubated with varying concentrations of curcumin and its analogues for 48 h and then examined for cell viability by the SRB assay. GI_{50} is the concentration of compounds that causes 50% inhibition compared to the vehicle control (0.25% DMSO). Samples were run in quintuplicate, and the results are the mean of at least two independent tests.

the third arylvinyl moiety. Importantly, the cytotoxic activity of these 4-arylidene curcumin analogues was not limited to A549 cells. In additional to A549 cells, other adenocarcinoma cells H1944, squamous cell carcinoma cells H157, and large cell carcinoma cells H460 were tested with selected 4-arylidene curcumin analogues. These compounds effectively decreased viability of all three major types of lung cancer cells tested. Most selected 4-arylidene analogues potently inhibited the growth of lung cancer cells with GI_{50} values at submicromolar concentrations (low to 0.07 μM) and induced apoptotic cell death. Data of representative compounds **17**, **21**, **35** are shown in Figure 2 (see Supporting Information for additional data from viability and apoptosis assays). These studies identified a new class of curcumin analogues with significantly improved activity against cancer cell growth.

Inhibition of TNFα Induced Nuclear Translocation of NF-κB by New Curcuminoids. One of the major curcumin targets critical for cancer survival is IκB kinase, IKK.[38] IKK is a key regulator of NF-κB activation. Activated NF-κB is localized at the nucleus to promote transcription, which can be triggered by TNFα.[39] Thus, we utilized nuclear translocation of NF-κB in response to TNFα as a primary readout to examine the mechanism of action of new curcuminoids in comparison to curcumin. An automated imaging system for high content analysis was employed to monitor the cytoplasmic/nuclear localization of NF-κB in response to TNFα.[37] A549 cells in a 384-well plate format were treated with various test compounds before TNFα was added to trigger the nuclear translocation of the NF-κB p65 subunit. As shown in Figure 3 and Table 2, curcumin (**1**) attenuated TNFα-induced nuclear redistribution of NF-κB with an IC_{50} of 11.6 μM, consistent with previous reports.[37]

The synthesized compounds were tested in the same assay and showed different degrees of activity against TNFα induced NF-κB activation. IC_{50} values of the tested curcuminoids are summarized in Table 2. As shown in Table 2, most of the traditional 1,3-diketones curcumin analogues (**2**−**4**, **6**) were less active than curcumin. Three monoketone curcumin analogues (**7**−**9**) showed improved activities (IC_{50} of 4.8−9.0 μM). Consistent with its cytotoxity profile, **10** was much less active (IC_{50} = 24.3 μM) than **7**-**9** in NF-κB inhibition,

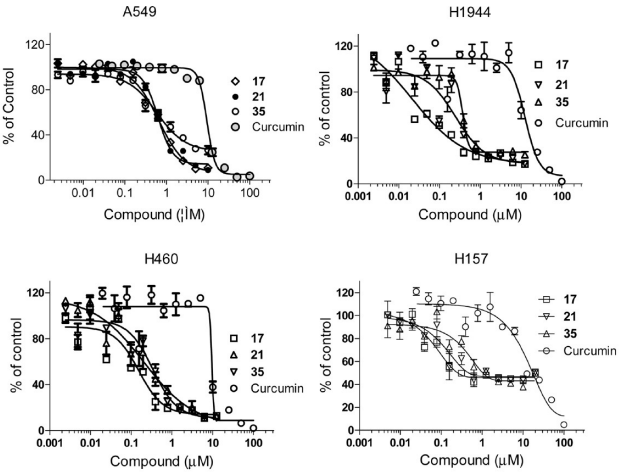

Compd.	Cell growth inhibition GI_{50} (μM)			
	A549	H1944	H460	H157
17	0.72	0.07	0.13	0.16
21	0.70	0.28	0.27	0.28
35	0.93	0.33	0.30	0.53
Curcumin	9.44	16.16	12.13	19.25

Figure 2. Inhibition of lung cancer cell viability by curcumin and its analogues. Cells were grown in 384-well plates and were treated with curcumin, **17**, **21**, or **35** as indicated for 72 h. Cell viability was assessed by the Alamar Blue method and expressed as % control (DMSO). Results with a panel of lung cancer cells are shown (lung adenocarcinoma, A549 H1944, H1792; squamous cell carcinoma, H157; squamous cell carcinoma, H157). Results from one representative experiment are shown.

indicating the disadvantages of thiophene replacement with respect to NF-κB inhibition.

Interestingly, except **19** and **30**, the newly designed 4-arylidene crucumin analogues (**13**−**37**) exhibited significant inhibitory activities against NF-κB translocation with IC_{50} values in the low micromolar range (1.0−4.9 μM). **17** (IC_{50} = 1.0 μM) and **21** (IC_{50} = 1.1 μM) showed more than 10-fold greater potency in blocking the nuclear localization of NF-κB than curcumin. The low activity of **19** may have resulted from its dimethylamine moiety, which might be protonized under the test conditions used, leading to unfavorable target interactions. **30**, however, remained unclear. Nevertheless, these synthesized 4-arylidene curcumin analogues generally showed superior activity to the classical 1,3-diketones analogues (**1**-**6**) while the monoketone analogues (**7**−**9**) displayed moderate activity, suggesting a strong correlation between a compound's molecular skeleton and its activity. From a comparison of the chemical structures of all three types of curcuminoids, the presence of absolute diketone moieties and 4-arylidene substitutions in **13**−**37** are unique over others (**1**−**7**, **9**, **10**). Both factors may contribute to the increased activities of the tested 4-arylidene curcumin analogues. To explore the nature of these phenomena, we further designed and evaluated the NF-κB inhibitory activity of 4-hydroxymethylene curcumin analogues **38**−**40**. **38**−**40** showed only poor inhibitory activity against NF-κB activation (Table 2), indicating the importance of the 4-arylidene substitution for activity. On the other hand, although the inhibitory activities varied, most of the triarylvinyl condensates

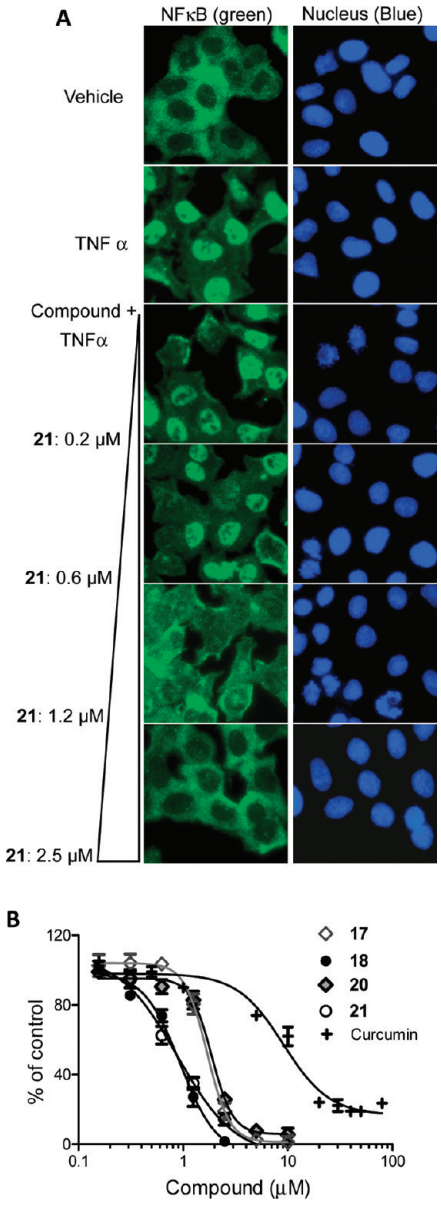

Figure 3. Inhibition of the TNFα induced NF-κB activation by new curcuminoids, **17**, **18**, **20**, and **21**. Results from one representative experiment are shown. (A) Example images of NF-κB subcellular localization. A549 cells were treated with compounds or vehicle (DMSO) for 30 min, followed by stimulation with TNFα (10 ng/mL) for 30 min. In the vehicle (DMSO) treatment, NF-κB is located at cytoplasm. Upon TNFα treatment, NF-κB is activated and translocated to the nucleus. Preincubation of the cells with increasing concentrations of compounds, with compound **21** as an example, dose-dependently inhibited the TNFα-induced NF-κB translocation to the nucleus. (B) Dose-response curves of the inhibitory effect of test compounds on TNFα-induced NF-κB activation. The inhibitory effect of the compound on TNFα induced NF-κB translocation (activation) was expressed as % of control = $\Delta FI_{(compound)}/\Delta FI_{(TNF\alpha\ only\ control)}$. ΔFI is the measured NF-κB fluorescence (green) intensity difference between nucleus and cytoplasm. Data shown are average values from triplicate samples with SD.

with different substituted groups (except **19** and **30**) were active at low micromolar concentrations. It might also be concluded that the triarylvinyl scaffolds of 4-arylidene curcumin analogues play a key role in their NF-κB inhibition activities as a pharmacophore, though further investigation is still needed to confirm that hypothesis.

Table 2. Inhibitory Effect of Compounds on NFκB Activation/Translocation[a]

	IC_{50} (μM)			IC_{50} (μM)			IC_{50} (μM)	
compd	mean	SD	compd	mean	SD	compd	mean	SD
curcumin	9.5	3.00	**16**	1.8	1.12	**29**	1.0	1.05
2	>40		**17**	1.0	0.55	**30**	>40	
3	>40		**18**	1.5	0.95	**31**	1.0	1.05
4	>40		**19**	>40		**32**	1.4	1.56
5	8.5	2.19	**20**	1.3	1.01	**33**	2.7	3.32
6	>40		**21**	1.1	0.45	**34**	1.8	2.14
7	7.9	4.26	**22**	1.4	0.26	**35**	1.7	1.0
8	4.8	1.85	**23**	1.4	1.48	**36**	1.3	1.35
9	9.0	3.44	**24**	4.9	1.96	**37**	2.8	1.02
10	24.3	7.01	**25**	1.5	0.04	**38**	39.3	
13	3.0	2.01	**26**	1.0	0.05	**39**	>40	
14	3.3	2.37	**27**	1.5	0.04	**40**	>40	
15	3.8	2.13	**28**	1.7	0.17			

[a] A549 cells were seeded in 384-well plates for 15 h, subsequently incubated with varying concentrations of curcumin and its analogues for 30 min and then stimulated with TNFα. The inhibitory effect of test compounds on TNFα induced NF-κB translocation was expressed as percentage of fluorescence intensity difference (in nucleus and in cytoplasm) in the control wells (TNFα only) after subtracting background (no TNFα treatment). The IC_{50} of NF-κB translocation stands for the concentration of a compound required to induce 50% inhibitory effect. Data points from each experiment were obtained as average values from triplicate samples. Data shown are the average from three independent experiments with standard deviation (SD).

Noticeably, the data in Tables 1 and 2 suggest an important correlation between the antiproliferative activity of tested compounds and their NF-κB inhibitory activity. Just like **1**−**6** and **10**, which showed low activities in both A549 cell growth and NF-κB activation inhibition, **7**−**9**, **38**−**40**, and most 4-arylidene curcumin analogues behaved consistently in both assays. These results strongly support the notion that the NF-κB pathway is one of the major molecular targets for curcumin and its analogues.

Enhanced Inhibition of IκB Kinase Activity by 4-Arylidene Curcumin Analogues. NF-κB is mainly activated by IKKβ in the well-defined canonical signaling pathway.[40] Because of this, we selected three potent curcumin analogues **17**, **21**, and **35** to directly test their effects on IKK enzymatic activity, with the parent compound curcumin as a control. Two assays were utilized: (i) a cell based IKK activation assay, which detects phosphorylated IκB and subsequent IκB degradation, and (ii) a reconstituted in vitro kinase assay which directly measures the transfer of γ-^{32}P from ATP to recombinant IκB. Upon stimulation of A549 cells with TNFα, activated IKKβ can catalyze the phosphorylation of IκB at Ser32 and Ser36, followed by degradation of phosphorylated IκB, leading the release and nuclear translocation of NF-κB. Antibodies against both IκB and Ser32 phosphorylated IκB were used to detect the status of IκB as a readout of IKK activity.

Figure 4 shows the Western blotting results of IκB phosphorylation (A) and subsequent degradation (B). Without the stimuli of TNFα, IκB showed a basal level of phosphorylation and no degradation (the first column). TNFα induced significant IκB phosphorylation and subsequent degradation of the protein (the second column). After treatment of cells with different compounds for 4 h, curcumin could block IκB phosphorylation and degradation when high concentrations were used, whereas **17**, **21**, and **35** potently block the IκB phosphorylation and degradation in a lower concentration. Dose-response curves for IκB phosphorylation suggested

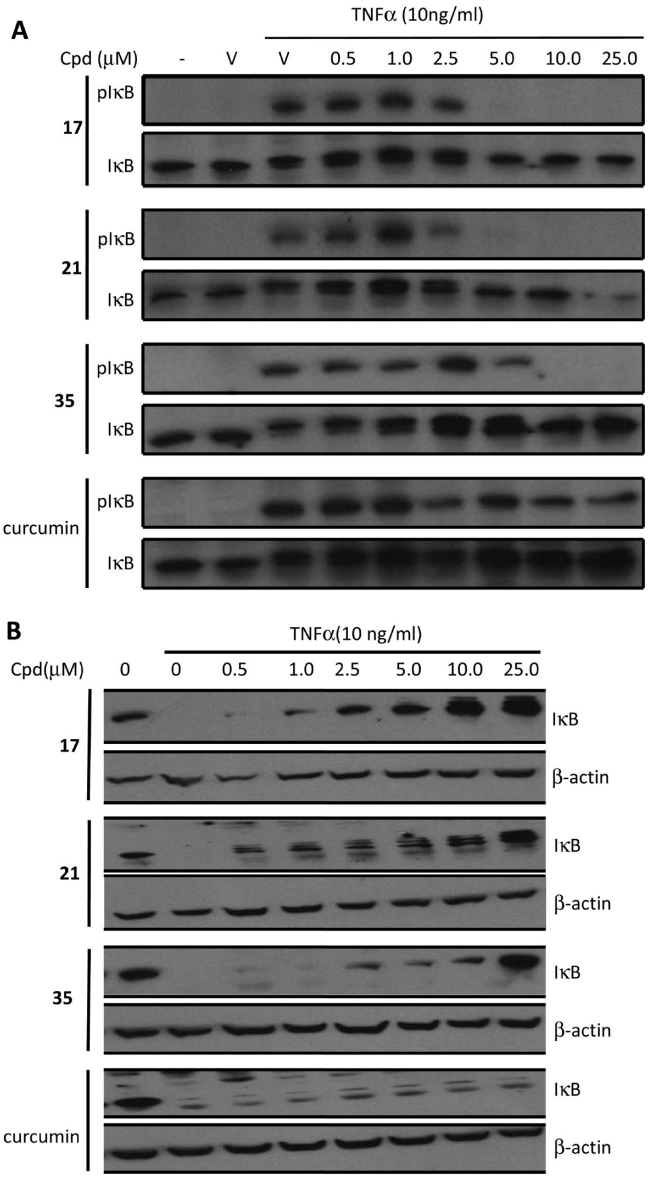

Figure 4. Effect of curcumin analogues on in vivo activity of IKK. (A) In vivo IKK activity as revealed by phosphorylation of IκB. A549 cells were pretreated with test compounds for 30 min prior to adding TNFα (10 ng/mL). Whole cell lysates were prepared after 7 min of TNFα treatment and analyzed for the phosphorylation state of IκB with anti-pS^{32} antibody via Western blotting. Then antibodies on the membrane were stripped and the membrane was reprobed for total IκB with antiserum against IκB as indicated. (B) IκB stability assay. A549 cells were pretreated with test compounds at indicated dosage prior to the addition of TNFα. Cells were cultured in the presence of TNFα (10 ng/mL) for an additional 20 min, lysed, and analyzed for total IκB levels by Western blot.

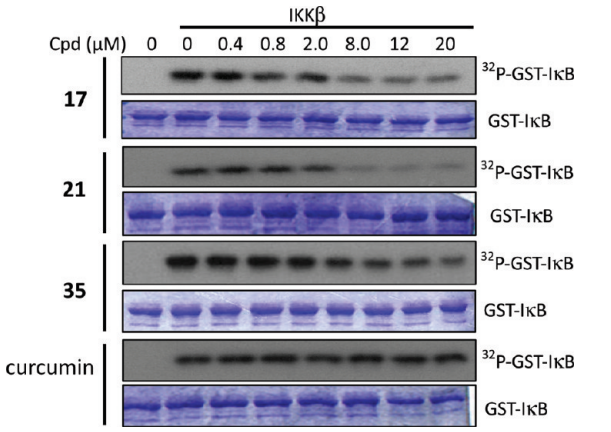

Figure 5. Effect of curcumin analogues on the catalytic activity of recombinant IKK in vitro. Recombinant IKKβ was incubated with increasing concentrations of test compounds as indicated. Addition of Mg/[γ-^{32}P] cocktail with purified GST-I-κB started the reactions, which were continued for 30 min at 30 °C. Proteins were separated by SDS−PAGE and processed for radiolabeled GST-I-κB (^{32}P-I-κB) and stained total GST-I-κB (GST- I-κB). Controls include reactions without IKKβ (lane 1 from left) or without compound (lane 2).

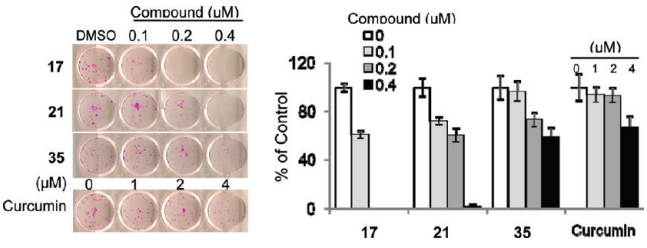

Figure 6. Compounds **17**, **21**, and **35** inhibit the colony formation of A549 cells. A549 cells were seeded in 12-well plate at a density of 200 cells/well and incubated overnight. The cells were then treated with compounds or vehicle (DMSO) for 3 days. The medium and compound were replaced for every 3 days. After a total of 9 days of incubation, cells were fixed and stained with SRB. The image of the plate was scanned, and the colonies were counted. (B) The colonies were counted and normalized to DMSO control. The data shown are the average of triplicate samples with SD.

IC_{50} values of 2.8 (**17**), 2.2 (**21**), and 5.0 μM (**35**), respectively, with a similar trend for IkB degradation. Those results suggest that **17**, **21**, and **35** block TNF-α induced NF-κB activation at least in part by inhibiting IκB phosphorylation and degradation. Again, the 4-arylidene curcumin analogues show much higher activities than curcumin.

The phosphorylation of IκB mainly depends on the IKKβ catalytic subunit of the IKK complex in the canonical pathway. It is possible that the inhibitory activities of curcumin and derivatives may be due to direct inhibition to the IKKβ kinase. To test this model, an in vitro reconstituted IKK inhibition assay was performed with recombinant IKKβ and its substrate GST-IκB.[37] The addition of curcumin in the range of tested concentrations had no obvious effect on IKKβ catalyzed incorporation of ^{32}P into its substrate GST-IκB (Figure 5). On the other hand, incubation of compounds **17**, **21**, and **35** induced a dose-dependent inhibition of IKKβ. Thus, the structural modifications of these novel curcumin analogues led to drastically enhanced inhibitory activity over curcumin in this defined in vitro IKK kinase assay.

Inhibition of Lung Cancer Clonogenic Activity by 4-Arylidene Curcumin Analogues. To compare the anticancer efficacy of curcumin and its new analogues, we investigated the effect of these compounds on colony formation properties of lung cancer cells, a readout for tumorigenesis.[41] A549 adenocarcinoma cells readily formed colonies in a solid matrix. The addition of the new triarylvinyl curcumin analogues **17**, **21**, and **35** drastically inhibited the number of colonies formed by A549 cells (Figure 6). At concentrations less than 0.2 μM, **17** and **21** reached ~50% inhibition, while **35** required approximately 0.4 μM to reach the same level of inhibition. For comparison, curcumin inhibited colony forming activity at much higher concentrations, with detectable inhibition at

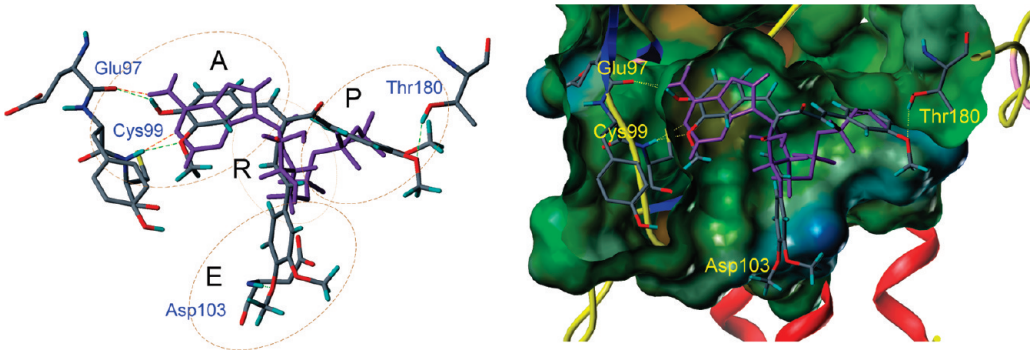

Figure 7. Binding of compound **17** and ATP with the IKKβ catalytic domain homology model. Left: Overlay of compound **17** (colored by atom type) and ATP (purple) in the ATP binding pocket. The molecules are represented in stick. Typical hydrogen bonds of compound **17** (green dotted line) and ATP (brown dotted line) with the homology model are shown. Right: Surface representation of the IKKβ catalytic domain homology model with compound **17** (colored by atom type) and ATP (purple) docking into the ATP binding pocket. The kinase surface was mapped by lipophilic potential (from orange to blue, lipophilic potential decrease) and Z-clipping to remove the N terminal region for visualization facility. Compound **17** adopts a propeller-shaped conformation in the pocket.

4 μM. These studies demonstrate that these 4-arylidene curcumin analogues have significantly improved anticancer activity over the parental curcumin.

Molecular Modeling of the IKKβ/17 Complex. To gain insights into the potential binding pose of the 4-arylidene curcumin analogues in IKKβ, a molecular docking analysis was carried out. Since three-dimensional structural data are unavailable for IKKβ, a homology model of the IKKβ catalytic domain was built based on four templates (PDB codes 2JC6, 1A06, 2QNJ, and 2A2A) from the Protein Data Bank (PDB) (see Experiments for details). Discovery Studio 2.1 (Accelrys Inc.) and Sybyl 7.3.5 (Tripos Inc.) were used for the homology model building and energy minimization of the IKKβ catalytic domain, respectively. The docking of the selected compound, **17**, to the IKKβ homology model suggests that **17** could potentially bind to the ATP pocket of IKKβ (Figure 7). Compound **17** adopts a propeller-shaped conformation in the pocket. The 4-arylidene moiety of **17** occupied the main hydrophobic adenine binding pockets (Figure 7, region A). The 4′-OH and 3′-OMe in 4-arylidene moiety of **17** have hydrogen bonds respectively with hinge region residues Glu97 and Cys99, which are the same residues targeted by the adenine moiety during the interaction of ATP with IKKβ catalytic domain. Furthermore, one of the 1,7-diaryl moieties of compound **17** lies along the phosphate binding pockets (Figure 7, region P) with a hydrogen bond between a 3′-OMe and residue Thr180. The other side of 1,7-diaryl moieties extends from the ribose binding pockets (Figure 7, region R) to the hydrophilic solvent-exposed entrance (Figure 7, region E), keeps orthogonal with the 4-arylidene moiety of **17**, and has a hydrogen bond between a 4′-OMe and residue Asp103 in the entrance region of the catalytic domain. It should be cautioned that this computer model provides a starting point, and details of the structure−activity relationship (SAR) have to be experimentally tested in future work.

In summary, our design and synthesis have led to the generation of a novel series of curcumin analogues. Biochemical and cell biology based studies coupled with high content analysis have led to the identification of a novel class of 4-arylidene curcumin analogues as a new generation of highly potent curcuminoids. These compounds exhibited significantly improved potency in blocking IKK activity and the NF-κB pathway as revealed by both in vivo and in vitro kinase assays and pathway analysis.

Consistent with their enhanced activity against a major molecular target, the representative 4-arylidene curcumin analogues effectively inhibited the viability of three types of lung cancer cells and attenuated the clonogenic activity of A549 cells. On the basis of our finding, it can be concluded that the triarylvinyl skeleton of 4-arylidene curcumin analogues acts as a phamacophore, and the 4-arylmethylene modification is an effective strategy to improve the NF-κB inhibitory activity of curcumin analogues.

Although presented data support an important role of IKKβ in the NF-κB pathway in mediating the effect of reported compounds, some observed differences in compound potency between cell viability assay and the IKKβ/NF-κB assays could be due to a number of factors. For example, (i) the status of compounds in cell culture and in vitro conditions could be different. The employed compounds could be further metabolized in cells to generate multiple active species, while in vitro kinase assays only measure the activity of the test compounds. (ii) Although IKKβ could be an important target of the tested curcumin analogues as proposed, the efficacy of the test compounds on cell survival is also determined by the cell's genetic background. Cells harboring different oncogene mutations, deletions, or amplifications could show different sensitivities to test compounds that target IKKβ. Our data in Figure 2 strongly support this model. (iii) The suppression of cell growth by these curcumin analogues could be due to their inhibition of other targets in addition to IKKβ. These potential targets include the cytoprotective antioxidant system. Whether and how these 4-arylidene curcumin analogues inhibit other targets in addition to IKKβ in cancer cells requires further investigation. Regardless, because of their potent IKKβ inhibitory activity, these novel triarylvinyl curcuminoids represent new opportunities for therapeutic development against cancer and other NF-κB dependent disorders, including various inflammatory diseases. Detailed SAR analysis is still required and is being actively pursued by our laboratory.

Experiments

General. All reagents used were commercially available. Solvents were treated using standard techniques. Reactions were monitored by TLC on a glass plate coated with silica gel with fluorescent indicator (GF_{254}). Column chromatography was performed on silica gel (100−200 mesh). ^{1}H NMR and ^{13}C NMR spectra were recorded with Varian INOVA 500NB or

Bruker Ultrashield 400 MHz spectrometer using TMS as an internal standard. Purity of target compounds was determined by reversed-phase HPLC analyses (Hypersil BDS-C18, 250 μm × 4.6 μm) with a flow rate of 0.5 mL/min. The samples were eluted with a gradient of constant 70% A (**2**−**4** and **40**), 90% A (**38** and **39**), or 50% A (others), where solvent A was CH_3CN and solvent B was 0.1% TFA in water, using UV monitor at 254 nm for detection. Retention times (t_R) were calculated in minutes, and purity was calculated as % total area. All compounds were >95% pure by HPLC. The HR-MS analysis was performed on a Thermo Finnigan MAT95XP-Trap instrument.

Chemistry. Synthesis of 1−10. 5-Hydroxy-1,7-bis(4-hydroxy-3-methoxyphenyl)hepta-1,4,6-trien-3-one (**1**), 5-hydroxy-1,7-bis(4- methoxyphenyl)hepta-1,4,6-trien-3-one (**2**), 1,7-bis(3,4-dimethoxyphenyl)-5-hydroxyhepta-1,4,6-trien-3-one (**3**), 5-hydroxy-1,7-bis(3,4,5-trimethoxyphenyl)hepta-1,4,6-trien-3-one (**4**), 5-hydroxy-1,7-bis(5-methylfuran-2-yl)hepta-1,4,6-trien-3-one (**5**), and 1,7-di(furan-2-yl)-5-hydroxyhepta-1,4,6-trien-3-one (**6**) were synthesized according to our previous report.[35]

(*E*)-4-(3,4,5-Trimethoxyphenyl)but-3-en-2-one (11) and (1*E*,4*E*)-1,5-Bis(3,4,5-trimethoxyphenyl)penta-1,4-dien-3-one (7). To a solution of 3 mL of acetone in 10 mL of EtOH, 0.84 g KOH (15 mmol, dissolved in 5 mL H_2O) was added at 0 °C, and the mixture was stirred for 20 min. After that, 2.94 g of 3,4,5-trimethoxybenzaldehyde (15 mmol, dissolved in 25 mL of EtOH) was added dropwise. Then the mixture was brought to room temperature for 2 h and monitored by TLC. Once the 3,4,5-trimethoxybenzaldehyde was consumed, the reaction solution was poured into water, and the resulting solution was neutralized by 2 N HCl. Then the raw product was extracted from water by acetic ether and purified with column chromatography (petroleum ether/acetic ether 5:1) to give 1.23 g of intermediate **11** (35%) and 1.53 g of yellow powder **7** (49%). HPLC t_R = 17.8 min; R_f = 0.38 (petroleum ether/acetic ether 2:1). ^{1}H NMR (400 MHz, $CDCl_3$) δ 7.65 (d, J = 15.8 Hz, 2H), 6.97 (d, J = 15.8 Hz, 2H), 6.84 (s, 4H), 3.91 (s, 12H), 3.89 (s, 6H). ^{13}C NMR (101 MHz, $CDCl_3$) δ 188.48, 153.51, 143.34, 140.52, 130.29, 124.82, 105.72, 61.00, 56.25.

(5*E*)-3-(3,4,5-Trimethoxybenzylidene)-6-(3,4,5-trimethoxyphenyl)hex-5-ene-2,4-dione (8). Compound **8** was synthesized in two steps. First the intermediate **12** was synthesized with the following procedures. Acetyl acetone (5.01 g, 50 mmol), boric anhydride (2.1 g, 30 mmol), and tri-*n*-butyl borate (23 g, 100 mmol) were mixed in ethyl acetate (100 mL) and stirred at 80 °C for 1 h. Then a solution of 3,4,5-trimethoxybenzaldehyde (1.96 g, 10 mmol) and *n*-butylamine (0.5 mL) in ethyl acetate was added dropwise in 1 h. Next the reaction mixture was stirred at room temperature for 2 days. The resulting solution was then neutralized by 0.4 N HCl and stirred for an additional 30 min in 60 °C. Then the raw product was extracted with ethyl acetate, and the organic layer was washed with water (30 mL, 2 times), dried (Na_2SO_4), and evaporated under vacuum. Finally the product was isolated by column chromatography (petroleum ether/acetic ether 9:1) to give 0.93 g intermediate **12** (33%). ^{1}H NMR (400 MHz, $CDCl_3$) δ 7.53 (d, J = 15.8 Hz, 1H), 6.77 (s, 2H), 6.39 (d, J = 15.8 Hz, 1H), 5.67 (s, 1H), 3.91 (s, 6H), 3.90 (s, 3H), 2.18 (s, 3H). After this, 557 mg of **12** (2 mmol) and 3,4,5-trimethoxybenzaldehyde (1.18 g, 6 mmol) were dissolved in 10 mL of DMF and stirred in 105 °C overnight. Then the DMF was evaporated under vacuum. Finally the crude mixture was purified with column chromatography (petroleum ether/acetic ether 5:1) to give 280 mg of **8** as a pale yellow powder, yield 31%. HPLC t_R = 11.1 min; R_f = 0.31 (petroleum ether/acetic ether 2:1). HRMS calcd for $C_{25}H_{28}O_8$: 456.1779, found 456.1780. ^{1}H NMR (400 MHz, $CDCl_3$) δ 7.64 (s, 1H), 7.40 (d, J = 16.1 Hz, 1H), 6.75 (d, J = 16.1 Hz, 1H), 6.71 (s, 2H), 6.68 (s, 2H), 3.87 (s, 3H), 3.85 (s, 6H), 3.84 (s, 3H), 3.79 (s, 6H), 2.41 (s, 3H). ^{13}C NMR (101 MHz, $CDCl_3$) δ 197.82, 195.75, 153.48, 153.19, 146.41, 141.04, 140.97, 140.36, 139.37, 129.35, 128.23, 126.27, 107.92, 105.91, 60.96, 60.90, 56.20, 56.14, 27.30.

General Procedure for the Synthesis of 9 and 10. 11 (236 mg, 1 mmol) and 1 mmol of the corresponding benzaldehyde were dissolved in 5 mL of EtOH, and KOH (56 mg, 1 mmol, dissolved in 0.1 mL H_2O) was added. The reaction mixture was stirred for 1 h at room temperature. Then the solution was poured into water and the resulting solution was neutralized by 2 N HCl. The raw product was extracted with ethyl acetate, and the organic layer was washed with water (10 mL, 2 times), dried (Na_2SO_4), and evaporated under vacuum. Finally the raw product was purified with column chromatography to give the final product.

(1*E*,4*E*)-1-(3,4-Dimethoxyphenyl)-5-(3,4,5-trimethoxyphenyl)-penta-1,4-dien-3-one (9). 3,4-dimethoxybenzaldehyde (166 mg, 1 mmol) was used as the benzaldehyde, and column chromatography (petroleum ether/acetic ether 2:1) gave 324 mg of **9** as a yellow powder, yield 84%. HPLC t_R = 13.5 min; R_f = 0.14 (petroleum ether/acetic ether 2:1). ^{1}H NMR (400 MHz, $CDCl_3$) δ 7.69 (d, J = 15.8 Hz, 1H), 7.64 (d, J = 15.8 Hz, 1H), 7.20 (dd, J = 1.9, 8.3 Hz, 1H), 7.13 (d, J = 1.9 Hz, 1H), 6.96 (d, J = 15.8 Hz, 1H), 6.95 (d, J = 15.8 Hz, 1H), 6.88 (d, J = 8.3 Hz, 1H), 6.84 (s, 2H), 3.93 (s, 3H), 3.92 (s, 3H), 3.90 (s, 6H), 3.89 (s, 3H). ^{13}C NMR (101 MHz, $CDCl_3$) δ 188.60, 153.51, 151.49, 149.33, 143.40, 143.03, 140.41, 130.41, 127.82, 125.00, 123.51, 123.21, 111.20, 110.04, 105.66, 61.02, 56.25, 56.03, 55.99.

(1*E*,4*E*)-1-(3-Methylthiophen-2-yl)-5-(3,4,5-trimethoxyphenyl)-penta-1,4-dien-3-one (10). 3-methylthiophene-2-carbaldehyde (126 mg, 1 mmol) was used as the benzaldehyde, and column chromatography (petroleum ether/acetic ether 9:1) gave 266 mg **10** as a yellow powder, yield 77%. HPLC t_R = 22.9 min; R_f = 0.39 (petroleum ether/acetic ether 3:1). HR-MS calcd for $C_{19}H_{20}O_4S_1$: 344.1077, found 344.1074. ^{1}H NMR (400 MHz, $CDCl_3$) δ 7.96 (d, J = 15.3 Hz, 1H), 7.63 (d, J = 15.9 Hz, 1H), 7.30 (d, J = 5.1 Hz, 1H), 6.91 (d, J = 5.1 Hz, 1H), 6.88 (d, J = 15.9 Hz, 1H), 6.86 (d, J = 15.3 Hz, 1H), 6.85 (s, 2H), 3.92 (s, 6H), 3.90 (s, 3H), 2.40 (s, 3H). ^{13}C NMR (101 MHz, $CDCl_3$) δ 188.07, 153.48, 142.94, 142.68, 134.48, 134.16, 131.48, 130.34, 127.29, 125.87, 122.85, 105.57, 61.00, 56.20, 14.32.

General Procedure for the Synthesis of 13−17, 19−28, and 30−37. An amount of 1.0 mmol of **1**, **2**, **3**, or **4** and 2 mmol of the corresponding benzaldehyde as well as 25 mL toluene were added to a three-neck rounded flask equipped with a water dispenser. Pyridine (4.0 mg, 0.05 mmol, in 0.1 mL toluene) and acetic acid (4.8 mg, 0.08 mmol, in 0.1 mL toluene) were added as catalysts. The reaction mixture was stirred in 140 °C overnight, and the generated water was removed by water dispenser during the whole reaction. Then the reaction mixture was washed with water (10 mL, twice) to remove pyridine and acetic acid. Next the organic layer was evaporated under vacuum to get raw product. Finally the product was purified by using silica gel column chromatography.

(1*E*,6*E*)-4-(4-Hydroxy-3-methoxybenzylidene)-1,7-bis(4-methoxyphenyl)hepta-1,6-diene-3,5-dione (13). 4-Hydroxy-3-methoxybenzaldehyde (304 mg, 2 mmol) and **2** (336 mg, 1 mmol) were used as reactants and the raw product was purified by column chromatograph (petroleum ether/acetic ether 2:1) to give 249 mg of **13** as a yellow powder, yield 53%. HPLC t_R = 19.5 min; R_f = 0.20 (petroleum ether/acetic ether 2:1). HR-MS calcd for $C_{29}H_{26}O_6$: 470.1724, found 470.1727. ^{1}H NMR (500 MHz, $CDCl_3$) δ 7.81 (s, 1H), 7.77 (d, J = 15.4 Hz, 1H), 7.53 (d, J = 16.1 Hz, 1H), 7.52 (d, J = 8.9 Hz, 2H), 7.42 (d, J = 8.8 Hz, 2H), 7.08 (dd, J = 2.0, 8.3 Hz, 1H), 7.03 (d, J = 2.0 Hz, 1H), 6.99 (d, J = 15.4 Hz, 1H), 6.89 (d, J = 8.8 Hz, 2H), 6.86 (d, J = 8.3 Hz, 1H), 6.86 (d, J = 8.9 Hz, 2H), 6.81 (d, J = 16.1 Hz, 1H), 3.83 (s, 3H), 3.81 (m, 6H). ^{13}C NMR (101 MHz, $CDCl_3$) δ 198.62, 186.81, 162.15, 161.79, 148.14, 146.64, 146.54, 144.48, 140.79, 138.69, 130.49, 130.42, 127.62, 126.90, 125.97, 125.75, 125.42, 120.11, 114.82, 114.50, 114.39, 112.45, 55.94, 55.41.

(1*E*,6*E*)-4-(3,4-Dimethoxybenzylidene)-1,7-bis(4-methoxyphenyl)-hepta-1,6-diene-3,5-dione (14). 3,4-Dimethoxybenzaldehyde (332 mg, 2 mmol) and **2** (336 mg, 1 mmol) were used as reactants and the raw product was purified by column chromatography

(petroleum ether/acetic ether 4:1) to give 312 mg of **14** as a yellow powder, yield 64%. HPLC t_R = 27.3 min; R_f = 0.33 (petroleum ether/acetic ether 2:1). HR-MS calcd for $C_{30}H_{28}O_6$: 484.1880, found 484.1886. ^{1}H NMR (500 MHz, $CDCl_3$) δ 7.82 (s, 1H), 7.78 (d, J = 15.4 Hz, 1H), 7.53 (d, J = 8.9 Hz, 2H), 7.53 (d, J = 15.4 Hz, 1H), 7.43 (d, J = 8.7 Hz, 2H), 7.13 (dd, J = 8.4, 1.8 Hz, 1H), 7.04 (d, J = 1.8 Hz, 1H), 6.99 (d, J = 15.4 Hz, 1H), 6.89 (d, J = 8.7 Hz, 2H), 6.86 (d, J = 8.9 Hz, 2H), 6.83 (d, J = 16.1 Hz, 1H), 6.82 (d, J = 8.4 Hz, 1H), 3.87 (s, 3H), 3.84 (s, 3H), 3.82 − 3.81 (m, 6H). ^{13}C NMR (101 MHz, $CDCl_3$) δ 198.73, 186.73, 162.13, 161.77, 151.09, 148.81, 146.81, 144.57, 140.65, 138.80, 130.53, 130.47, 127.52, 126.79, 126.31, 125.35, 125.05, 119.95, 114.47, 114.35, 112.82, 111.02, 55.90, 55.82, 55.43, 55.40.

(1*E*,6*E*)-1,7-Bis(4-methoxyphenyl)-4-(2,3,4-trimethoxybenzylidene)hepta-1,6-diene-3,5-dione (15). 3,4,5-Trimethoxybenzaldehyde (392 mg, 2 mmol) and **2** (336 mg, 1 mmol) were used as reactants and the raw product was purified by column chromatography (petroleum ether/acetic ether 4:1) to give 283 mg of **15** as a yellow powder, yield 55%. HPLC t_R = 32.0 min; R_f = 0.39 (petroleum ether/acetic ether 2:1). HR-MS calcd for $C_{31}H_{30}O_7$: 514.1986, found 514.1987. ^{1}H NMR (500 MHz, $CDCl_3$) δ 7.78 (d, J = 15.4 Hz, 1H), 7.76 (s, 1H), 7.53 (d, J = 8.7 Hz, 2H), 7.53 (d, J = 16.1 Hz, 1H), 7.43 (d, J = 8.7 Hz, 2H), 6.98 (d, J = 15.4 Hz, 1H), 6.90 (d, J = 8.8 Hz, 2H), 6.87 (d, J = 8.8 Hz, 2H), 6.81 (d, J = 16.1 Hz, 1H), 6.76 (s, 2H), 3.84 (m, 6H), 3.82 (s, 3H), 3.80 (s, 6H). ^{13}C NMR (101 MHz, $CDCl_3$) δ 198.24, 186.77, 162.23, 161.89, 153.13, 146.82, 144.94, 140.46, 140.28, 140.10, 130.54, 128.87, 127.47, 126.76, 125.26, 119.88, 114.54, 114.41, 107.92, 60.93, 56.14, 55.45, 55.43.

(1*E*,6*E*)-1,7-Bis(3,4-dimethoxyphenyl)-4-(3,4,5-trimethoxybenzylidene)hepta-1,6-diene-3,5-dione (16). 3,4,5-Trimethoxybenzaldehyde (392 mg, 2 mmol) and **3** (396 mg, 1 mmol) were used as reactants and the raw product was purified by column chromatography (petroleum ether/acetic ether 2:1) to give 486 mg of **16** as a yellow powder, yield 85%. HPLC t_R = 17.0 min; R_f = 0.39 (petroleum ether/acetic ether 1:1). HR-MS calcd for $C_{33}H_{34}O_9$: 574.2197, found 574.2201. ^{1}H NMR (500 MHz, $CDCl_3$) δ 7.75 (s, 1H), 7.76 (d, J = 15.4 Hz, 1H), 7.51 (d, J = 16.1 Hz, 1H), 7.18 (dd, J = 8.4, 2.0 Hz, 1H), 7.07 (d, J = 2.0 Hz, 1H), 7.05 (dd, J = 8.4, 2.0 Hz, 1H), 6.98 (d, J = 2.0 Hz, 1H), 6.98 (d, J = 15.4 Hz, 1H), 6.86 (d, J = 8.4 Hz, 1H), 6.82 (d, J = 8.4 Hz, 1H), 6.80 (d, J = 16.1 Hz, 1H), 6.76 (s, 2H) 3.90 (s, 3H), 3.89(s, 3H), 3.88(s, 3H), 3.86 (s, 3H), 3.84 (s, 3H), 3.78 (s, 6H). ^{13}C NMR (101 MHz, $CDCl_3$) δ 197.96, 186.86, 153.18, 152.10, 151.78, 149.42, 149.33, 146.96, 145.23, 140.46, 140.40, 140.27, 128.84, 127.77, 127.07, 125.48, 123.56, 123.37, 120.21, 111.24, 110.76, 110.33, 108.02, 60.89, 56.17, 56.02, 55.97.

(1*E*,6*E*)-1,7-Bis(3,4-dimethoxyphenyl)-4-(4-hydroxy-3-methoxybenzylidene)hepta-1,6-diene-3,5-dione (17). 4-Hydroxy-3-methoxybenzaldehyde (304 mg, 2 mmol) and **3** (396 mg, 1 mmol) were used as reactants and the raw product was purified by column chromatography (petroleum ether/acetic ether 2:1) to give 320 mg of **17** as a yellow powder, yield 60%. HPLC t_R = 11.6 min; R_f = 0.27 (petroleum ether/acetic ether 1:1). HR-MS calcd for $C_{31}H_{30}O_8$: 530.1935, found 530.1941. ^{1}H NMR (500 MHz, $CDCl_3$) δ 7.80 (s, 1H), 7.75 (d, J = 15.4 Hz, 1H), 7.50 (d, J = 16.1 Hz, 1H), 7.18 (dd, J = 8.5, 2.0 Hz, 1H), 7.09 (dd, J = 8.5, 2.0 Hz, 1H), 7.06 (dd, J = 8.0, 2.0 Hz, 1H), 7.06 (d, J = 2.0 Hz, 1H), 7.04 (d, J = 2.0 Hz, 1H), 6.98 (d, J = 2.0 Hz, 1H), 6.97 (d, J = 15.4 Hz, 1H), 6.87 (d, J = 8.5 Hz, 1H), 6.86 (d, J = 8.0 Hz, 1H), 6.82 (d, J = 8.5 Hz, 1H), 6.81 (d, J = 16.1 Hz, 1H), 3.91 (m, 6H), 3.89 (s, 3H), 3.87 (s, 3H), 3.83 (s, 3H). ^{13}C NMR (101 MHz, $CDCl_3$) δ 198.61, 186.89, 151.96, 151.61, 149.31, 149.24, 148.17, 147.02, 146.54, 144.92, 140.96, 138.58, 127.81, 127.09, 125.90, 125.71, 125.57, 123.60, 123.31, 120.20, 114.84, 112.42, 111.15, 111.12, 110.61, 110.19, 56.04, 56.03, 56.01, 55.94.

(1*E*,6*E*)-1,7-Bis(3,4-dimethoxyphenyl)-4-(4-(dimethylamino)benzylidene)hepta-1,6-diene-3,5-dione (19). 4-(Dimethylamino)benzaldehyde (298 mg, 2 mmol) and **3** (396 mg, 1 mmol) were used as reactants and the raw product was purified by column chromatography (petroleum ether/acetic ether 2:1) to give 258 mg of **19** as a red powder, yield 49%. HPLC t_R = 18.1 min; R_f = 0.39 (petroleum ether/acetic ether 1:1). HR-MS calcd for $C_{32}H_{33}O_6N_1$: 527.2302, found 527.2301. ^{1}H NMR (500 MHz, $CDCl_3$) δ 7.73 (d, J = 15.4 Hz, 1H), 7.52 (d, J = 16.0 Hz, 1H), 7.42 (d, J = 8.9 Hz, 2H), 7.17 (dd, J = 8.4, 1.8 Hz, 1H), 7.07 (dd, J = 8.5, 1.9 Hz, 1H), 7.06 (d, J = 1.8 Hz, 1H), 7.00 (d, J = 1.9 Hz, 1H), 6.99 (d, J = 15.4 Hz, 1H), 6.84 (d, J = 8.5 Hz, 1H), 6.85 (d, J = 16.0 Hz, 1H), 6.81 (d, J = 8.4 Hz, 1H), 6.61 (d, J = 8.9 Hz, 2H), 3.90 (s, 3H), 3.90 (s, 3H), 3.88 (s, 3H), 3.86 (s, 3H), 2.99 (s, 6H). ^{13}C NMR (101 MHz, $CDCl_3$) δ 199.52, 186.63, 151.80, 151.69, 151.33, 149.23, 149.20, 146.50, 143.88, 142.14, 135.43, 133.08, 128.14, 127.43, 126.16, 123.47, 123.05, 120.87, 120.72, 111.66, 111.15, 111.06, 110.62, 110.28, 56.06, 56.02, 56.01, 55.93, 39.97.

(1*E*,6*E*)-1,7-Bis(3,4-dimethoxyphenyl)-4-(3-fluorobenzylidene)hepta-1,6-diene-3,5-dione (20). 3-Fluorobenzaldehyde (248 mg, 2 mmol) and **3** (396 mg, 1 mmol) were used as reactants and the raw product was purified by column chromatography (petroleum ether/acetic ether 3:1) to give 413 mg of **20** as a yellow powder, yield 82%. HPLC t_R = 22.5 min; R_f = 0.36 (petroleum ether/acetic ether 3:2). HR-MS calcd for $C_{30}H_{27}O_6F_1$: 502.1786, found 502.1785. ^{1}H NMR (400 MHz, $CDCl_3$) δ 7.80 (d, J = 15.4 Hz, 1H), 7.78 (s, 1H), 7.46 (d, J = 16.2 Hz, 1H), 7.30 (dd, J = 8.0, 7.5 Hz, 1H), 7.29 (d, J = 8.0 Hz, 1H), 7.21 (d, J = 1.8 Hz, 1H), 7.19 (d, J = 1.8 Hz, 1H), 7.10−7.04 (m, 2H), 7.03 (dd, J = 8.3 Hz, J = 1.8 Hz, 1H), 6.99 (s, 1H), 6.95 (d, J = 15.4 Hz, 1H), 6.87 (d, J = 8.3 Hz, 1H), 6.84 (d, J = 8.3 Hz, 1H), 6.80 (d, J = 16.2 Hz, 1H), 3.92 (s, 6H), 3.90 (s, 3H), 3.88 (s, 3H). ^{13}C NMR (101 MHz, $CDCl_3$) δ 197.47, 186.74, 162.68 (d, J = 247.2 Hz), 152.09, 151.83, 149.29, 149.24, 147.83, 145.92, 141.94, 138.75, 135.71 (d, J = 7.9 Hz), 130.39 (d, J = 8.3 Hz), 127.54, 126.89, 126.06 (d, J = 2.9 Hz), 125.40, 123.85, 123.62, 119.84, 117.16 (d, J = 21.4 Hz), 116.60 (d, J = 22.3 Hz), 111.10, 111.04, 110.54, 110.04, 56.05, 56.04, 55.93.

(1*E*,6*E*)-1,7-Bis(3,4-dimethoxyphenyl)-4-(4-fluorobenzylidene)hepta-1,6-diene-3,5-dione (21). 4-Fluorobenzaldehyde (248 mg, 2 mmol) and **3** (396 mg, 1 mmol) were used as reactants and the raw product was purified by column chromatography (petroleum ether/acetic ether 3:1) to give 390 mg of **21** as a yellow powder, yield 78%. HPLC t_R = 21.9 min; R_f = 0.33 (petroleum ether/acetic ether 3:2). HR-MS calcd for $C_{30}H_{27}O_6F_1$: 502.1786, found 502.1789. ^{1}H NMR (400 MHz, $CDCl_3$) δ 7.81 (s, 1H), 7.78 (d, J = 15.4 Hz, 1H), 7.48−7.51 (m, 2H), 7.47 (d, J = 16.2 Hz, 1H), 7.19 (dd, J = 8.4, 2.0 Hz, 1H), 7.05−7.06 (m, 2H), 7.03 (d, J = 8.7 Hz, 1H), 7.01 (d, J = 8.6 Hz, 1H), 6.99 (d, J = 2.0 Hz, 1H), 6.96 (d, J = 15.4 Hz, 1H), 6.87 (d, J = 8.3 Hz, 1H), 6.83 (d, J = 8.4 Hz, 1H), 6.80 (d, J = 16.2 Hz, 1H), 3.92 (s, 3H), 3.91 (s, 3H), 3.89 (s, 3H), 3.88 (s, 3H). ^{13}C NMR (101 MHz, $CDCl_3$) δ 197.92, 186.76, 163.73 (d, J = 252.5 Hz), 152.09, 151.77, 149.32, 149.25, 147.63, 145.59, 140.57, 139.18, 132.38 (d, J = 8.6 Hz), 129.79 (d, J = 3.3 Hz), 127.63, 126.93, 125.43, 123.79, 123.52, 119.97, 116.07 (d, J = 21.9 Hz), 111.12, 111.07, 110.58, 110.09, 56.06, 56.04, 55.94.

(1*E*,6*E*)-1,7-Bis(3,4-dimethoxyphenyl)-4-(4-hydroxybenzylidene)hepta-1,6-diene-3,5-dione (22). 4-Hydroxybenzaldehyde (244 mg, 2 mmol) and **3** (396 mg, 1 mmol) were used as reactants and the raw product was purified by column chromatography (petroleum ether/acetic ether 2:1) to give 187 mg of **22** as an orange powder, yield 37%. HPLC t_R = 11.6 min; R_f = 0.30 (petroleum ether/acetic ether 1:1). HR-MS calcd for $C_{30}H_{28}O_7$: 500.1830, found 500.1826. ^{1}H NMR (400 MHz, DMSO) δ 7.76 (d, J = 15.4 Hz, 1H), 7.50 (d, J = 16.1 Hz, 1H), 7.39 (d, J = 8.7 Hz, 2H), 7.19 (dd, J = 8.4, 1.9 Hz, 1H), 7.06 (d, J = 1.9 Hz, 1H), 7.07 (dd, J = 8.2, 2.1 Hz, 1H), 7.00 (d, J = 2.1 Hz, 1H), 6.97 (d, J = 15.4 Hz, 1H), 6.86 (d, J = 8.4 Hz, 1H), 6.83 (d, J = 8.4 Hz, 1H), 6.83 (d, J = 16.1 Hz, 1H), 6.78 (d, J = 8.7 Hz, 2H), 3.92 (s, 3H), 3.91 (s, 3H), 3.89 (s, 3H), 3.87 (s, 3H). ^{13}C NMR (101 MHz, DMSO) δ 198.22, 187.83, 159.85, 151.39, 151.14, 148.95, 148.93, 145.93, 143.26, 140.22, 137.93, 132.55, 127.48, 126.78, 125.42, 124.23, 123.51, 123.29, 119.29, 115.81, 111.62, 111.49, 111.16, 110.68, 55.71, 55.54.

(1*E*,6*E*)-4-(2,5-Dimethoxybenzylidene)-1,7-bis(4-hydroxy-3-methoxyphenyl)hepta-1,6-diene-3,5-dione (23). 2,5-Dimethoxybenzaldehyde (332 mg, 2 mmol) and **1** (368 mg, 1 mmol) were used as reactants, and column chromatography (petroleum ether/acetic ether 2:1) gave 177 mg of **23** as a yellow powder, yield 34%. HPLC t_R = 10.7 min; R_f = 0.20 (petroleum ether/acetic ether 1:1). HR-MS calcd for $C_{30}H_{28}O_8[M - H]^-$: 515.1706, found 515.1701. ^{1}H NMR (400 MHz, $CDCl_3$) δ 8.14 (s, 1H), 7.74 (d, J = 15.5 Hz, 1H), 7.44 (d, J = 16.1 Hz, 1H), 7.17 (dd, J = 8.2, 1.8 Hz, 1H), 7.05 (d, J = 1.8 Hz, 1H), 7.01 (d, J = 15.5 Hz, 1H), 6.99 (dd, J = 8.1, 1.9 Hz, 1H), 6.94−6.95 (m, 2H), 6.92 (d, J = 8.2 Hz, 1H), 6.84−6.87 (m, 2H), 6.80 (d, J = 9.0 Hz, 1H), 6.70 (d, J = 16.1 Hz, 1H), 5.92 (s, 1H), 5.92 (s, 1H), 3.93 (s, 3H), 3.88 (s, 3H), 3.84 (s, 3H), 3.67 (s, 3H). ^{13}C NMR (400 MHz, $CDCl_3$) δ197.61, 187.76, 153.21, 152.49, 148.63, 148.41, 146.76, 145.17, 140.88, 136.27, 127.41, 126.87, 125.31, 123.96, 123.58, 123.43, 120.15, 117.70, 114.91, 114.83, 114.76, 111.92, 110.31, 109.72, 56.05, 56.01, 55.95, 55.74.

(1*E*,6*E*)-1,7-Bis(3,4-dimethoxyphenyl)-4-(4-ethylbenzylidene)-hepta-1,6-diene-3,5-dione (24). 4-Ethylbenzaldehyde (268 mg, 2 mmol) and **3** (396 mg, 1 mmol) were used as reactants and the raw product was purified by column chromatography (petroleum ether/acetic ether 4:1) to give 316 mg of **24** as a yellow powder, yield 62%. HPLC t_R = 27.9 min; R_f = 0.37 (petroleum ether/acetic ether 3:2). HR-MS calcd for $C_{32}H_{32}O_6$: 512.2193, found 512.2196. ^{1}H NMR (400 MHz, $CDCl_3$) δ 7.85 (s, 1H), 7.78 (d, J = 15.4 Hz, 1H), 7.49 (d, J = 16.2 Hz, 1H), 7.43 (d, J = 8.2 Hz, 2H), 7.19 (dd, J = 8.5, 1.9 Hz, 1H), 7.16 (d, J = 8.2 Hz, 2H), 7.07 (d, J = 1.9 Hz, 1H), 7.06 (dd, J = 8.3, 1.8 Hz, 1H), 6.99 (d, J = 1.8 Hz, 1H), 7.00 (d, J = 15.4 Hz, 1H), 6.86 (d, J = 8.3 Hz, 1H), 6.82 (d, J = 8.5 Hz, 1H), 6.83 (d, J = 16.2 Hz, 1H), 3.91 (s, 6H), 3.88 (s, 3H), 3.87 (s, 3H), 2.62 (q, J = 7.6 Hz, 2H), 1.19 (t, J = 7.6 Hz, 3H). ^{13}C NMR (101 MHz, $CDCl_3$) δ 198.33, 187.04, 151.85, 151.60, 149.20, 149.18, 147.21, 147.17, 145.18, 140.76, 139.81, 130.87, 130.61, 130.23, 128.40, 127.92, 127.71, 127.10, 125.67, 123.64, 123.39, 120.08, 111.08, 110.99, 110.51, 110.09, 55.99, 55.88, 28.74, 15.09.

(1*E*,6*E*)-4-(2,3-Dimethoxybenzylidene)-1,7-bis(3,4-dimethoxyphenyl)hepta-1,6-diene-3,5-dione (25). 2,3-Dimethoxybenzaldehyde (332 mg, 2 mmol) and **3** (396 mg, 1 mmol) were used as reactants and the raw product was purified by column chromatography (petroleum ether/acetic ether 3:1) to give 225 mg of **25** as a yellow powder, yield 41%. HPLC t_R = 21.0 min; R_f = 0.26 (petroleum ether/acetic ether 3:2). HR-MS calcd for $C_{32}H_{32}O_8$: 544.2092, found 544.2090. ^{1}H NMR (400 MHz, $CDCl_3$) δ 8.14 (s, 1H), 7.77 (d, J = 15.4 Hz, 1H), 7.43 (d, J = 16.1 Hz, 1H), 7.20 (dd, J = 8.3, 1.9 Hz, 1H), 7.08 (d, J = 1.9 Hz, 1H), 7.02 (dd, J = 8.4, 1.9 Hz, 1H), 7.01 (d, J = 15.4 Hz, 1H), 6.98 (dd, J = 7.8, 1.8 Hz, 1H), 6.96 (d, J = 1.9 Hz, 1H), 6.95 (t, J = 7.8 Hz, 1H), 6.90 (dd, J = 7.8, 1.8 Hz, 1H), 6.87 (d, J = 8.4 Hz, 1H), 6.81 (d, J = 8.3 Hz, 1H), 6.72 (d, J = 16.1 Hz, 1H), 3.93−3.90 (m, 9H), 3.89 (s, 3H), 3.86 (s, 3H), 3.84 (s, 3H). ^{13}C NMR (101 MHz, $CDCl_3$) δ 197.35, 187.65, 152.70, 151.77, 151.65, 149.25, 148.34, 146.66, 145.20, 141.65, 136.09, 128.30, 127.79, 127.27, 125.78, 124.10, 123.51, 123.38, 121.89, 120.42, 114.42, 111.16, 111.06, 110.54, 110.06, 61.35, 56.01, 55.90, 55.86.

(1*E*,6*E*)-4-(3,4-Dimethoxybenzylidene)-1,7-bis(3,4,5-trimethoxyphenyl)hepta-1,6-diene-3,5-dione (26). 3,4-Dimethoxybenzaldehyde (332 mg, 2 mmol) and **4** (456 mg, 1 mmol) were used as reactants and the raw product was purified by column chromatography (petroleum ether/acetic ether 3:2) to give 323 mg of **26** as a yellow powder, yield 53%. HPLC t_R = 18.6 min; R_f = 0.16 (petroleum ether/acetic ether 3:2). HR-MS calcd for $C_{34}H_{36}O_{10}$: 604.2303, found 604.2313. ^{1}H NMR (500 MHz, $CDCl_3$) δ 7.82 (s, 1H), 7.72 (d, J = 15.5 Hz, 1H), 7.47 (d, J = 16.1 Hz, 1H), 7.13 (dd, J = 8.5, 2.0 Hz, 1H), 7.04 (d, J = 2.0 Hz, 1H), 7.02 (d, J = 15.5 Hz, 1H), 6.83 (d, J = 8.5 Hz, 1H), 6.83 (d, J = 16.1 Hz, 1H), 6.80 (s, 2H), 6.70 (s, 2H), 3.89 (s, 6H), 3.88 (s, 3H), 3.88 (s, 3H), 3.86 (s, 3H), 3.84 (s, 6H), 3.82 (s, 3H). ^{13}C NMR (101 MHz, $CDCl_3$) δ 198.25, 186.95, 153.53, 151.43, 149.05, 146.86, 145.03, 141.21, 140.95, 138.79, 130.24, 129.51, 126.87, 126.27, 125.07, 121.54, 113.04, 111.24, 106.24, 106.13, 60.99, 56.38, 56.27, 55.97, 55.93.

(1*E*,6*E*)-4-(2,5-Dimethoxybenzylidene)-1,7-bis(3,4-dimethoxyphenyl)hepta-1,6-diene-3,5-dione (27). 2,5-Dimethoxybenzaldehyde (332 mg, 2 mmol) and **3** (396 mg, 1 mmol) were used as reactants and the raw product was purified by column chromatography (petroleum ether/acetic ether 3:1) to give 211 mg of **27** as a yellow powder, yield 39%. HPLC t_R = 20.4 min; R_f = 0.24 (petroleum ether/acetic ether 3:2). HR-MS calcd for $C_{32}H_{32}O_8$: 544.2092, found 544.2096. ^{1}H NMR (400 MHz, $CDCl_3$) δ 8.15 (s, 1H), 7.76 (d, J = 15.5 Hz, 1H), 7.46 (d, J = 16.1 Hz, 1H), 7.20 (dd, J = 8.3, 1.5 Hz, 1H), 7.09 (d, J = 1.5 Hz, 1H), 7.03 (dd, J = 8.0, 1.5 Hz, 1H), 7.04 (d, J = 15.5 Hz, 1H), 6.95−6.96 (m, 2H), 6.87 (d, J = 8.3 Hz, 1H), 6.85−6.87 (m, 1H), 6.82 (d, J = 8.0 Hz, 1H), 6.80 (d, J = 8.8 Hz, 1H), 6.73 (d, J = 16.1 Hz, 1H), 3.92 (s, 6H), 3.89 (s, 3H), 3.87 (s, 3H), 3.84 (s, 3H), 3.67 (s, 3H). ^{13}C NMR (101 MHz, $CDCl_3$) δ 197.49, 187.78, 153.20, 152.46, 151.70, 151.54, 149.18, 146.47, 144.96, 140.90, 136.31, 127.78, 127.25, 125.53, 123.48, 123.39, 123.30, 120.38, 117.67, 114.94, 111.91, 111.11, 111.02, 110.47, 109.97, 55.98, 55.88, 55.70.

(1*E*,6*E*)-4-(2,4-Dimethoxybenzylidene)-1,7-bis(3,4-dimethoxyphenyl)hepta-1,6-diene-3,5-dione (28). 2,4-Dimethoxybenzaldehyde (332 mg, 2 mmol) and **3** (396 mg, 1 mmol) were used as reactants and the raw product was purified by column chromatography (petroleum ether/acetic ether 3:1) to give 337 mg of **28** as a yellow powder, yield 62%. HPLC t_R = 19.7 min; R_f = 0.40 (petroleum ether/acetic ether 1:1). HR-MS calcd for $C_{32}H_{32}O_8$: 544.2092, found 544.2094. ^{1}H NMR (400 MHz, $CDCl_3$) δ 8.20 (s, 1H), 7.74 (d, J = 15.5 Hz, 1H), 7.48 (d, J = 16.1 Hz, 1H), 7.36 (d, J = 8.4 Hz, 1H), 7.19 (dd, J = 8.3, 1.8 Hz, 1H), 7.08 (d, J = 1.8 Hz, 1H), 7.05 (dd, J = 8.3, 1.8 Hz, 1H), 7.03 (d, J = 15.5 Hz, 1H), 6.98 (d, J = 1.8 Hz, 1H), 6.87 (d, J = 8.3 Hz, 1H), 6.82 (d, J = 8.3 Hz, 1H), 6.75 (d, J = 16.1 Hz, 1H), 6.41 (d, J = 2.4 Hz, 1H), 6.40 (dd, J = 8.4, 2.4 Hz, 1H), 3.91 (s, 6H), 3.89 (s, 3H), 3.87 (s, 6H), 3.79 (s, 3H). ^{13}C NMR (101 MHz, $CDCl_3$) δ 198.32, 187.60, 163.17, 159.83, 151.62, 151.37, 149.17, 149.15, 146.10, 144.34, 138.40, 136.26, 131.78, 127.96, 127.37, 125.73, 123.41, 123.10, 120.62, 115.80, 111.09, 111.00, 110.52, 110.04, 105.16, 98.27, 55.99, 55.89, 55.53, 55.43.

(1*E*,6*E*)-4-(3,4-Dimethoxybenzylidene)-1,7-bis(4-hydroxy-3-methoxyphenyl)hepta-1,6-diene-3,5-dione (30). 3,4-Dimethoxybenzaldehyde (332 mg, 2 mmol) and **1** (368 mg, 1 mmol) were used as reactants, and column chromatography (petroleum ether/acetic ether 3:2) gave 347 mg of **30** as a yellow powder, yield 67%. HPLC t_R = 9.3 min; R_f = 0.20 (petroleum ether/acetic ether 1:1). HR-MS calcd for $C_{30}H_{28}O_8$: 516.1779, found 516.1783. ^{1}H NMR (400 MHz, $CDCl_3$) δ 7.81 (s, 1H), 7.77 (d, J = 15.4 Hz, 1H), 7.49 (d, J = 16.1 Hz, 1H), 7.16 (dd, J = 8.4, 1.9 Hz, 1H), 7.14 (dd, J = 8.2, 2.0 Hz, 1H), 7.03−7.06 (m, 2H), 7.03 (dd, J = 8.2, 1.9 Hz, 1H), 6.97 (d, J = 1.9 Hz, 1H), 6.96 (d, J = 15.4 Hz, 1H), 6.91 (d, J = 8.2 Hz, 1H), 6.88 (d, J = 8.2 Hz, 1H), 6.82 (d, J = 8.4 Hz, 1H), 6.81 (d, J = 16.1 Hz, 1H), 5.96 (s, 1H), 5.94 (s, 1H), 3.92 (s, 3H), 3.89 (s, 3H), 3.87 (s, 3H), 3.82 (s, 3H). ^{13}C NMR (101 MHz, $CDCl_3$) δ 198.79, 186.90, 151.13, 148.98, 148.83, 148.55, 147.49, 146.91, 146.83, 145.25, 140.74, 138.74, 127.31, 126.57, 126.28, 125.20, 125.02, 124.04, 123.59, 119.76, 114.94, 114.91, 112.84, 111.05, 110.44, 109.99, 56.04, 55.95, 55.91, 55.84.

(1*E*,6*E*)-4-(2,4-Dimethoxybenzylidene)-1,7-bis(4-hydroxy-3-methoxyphenyl)hepta-1,6-diene-3,5-dione (31). 2,4-Dimethoxybenzaldehyde (332 mg, 2 mmol) and **1** (368 mg, 1 mmol) were used as reactants, and column chromatography (petroleum ether/acetic ether 2:1) gave 268 mg of **31** as a yellow powder, yield 52%. HPLC t_R = 11.1 min; R_f = 0.29 (petroleum ether/acetic ether 1:1). HR-MS calcd for $C_{30}H_{28}O_8$: 516.1779, found 516.1782. ^{1}H NMR (400 MHz, $CDCl_3$) δ 8.19 (s, 1H), 7.72 (d, J = 15.4 Hz, 1H), 7.45 (d, J = 16.1 Hz, 1H), 7.35 (d, J = 8.4 Hz, 1H), 7.17 (d, J = 8.4 Hz, 1H), 7.05 (s, 1H), 7.01 (d, J = 8.4 Hz, 1H), 7.00 (d, J = 15.4 Hz, 1H), 6.96 (s, 1H), 6.91 (d, J = 8.2 Hz, 1H), 6.87 (d, J = 8.2 Hz, 1H), 6.73 (d, J = 16.1 Hz, 1H), 6.41

(s, 1H), 6.39 (d, J = 8.4 Hz, 1H), 5.89 (m, 2H), 3.93 (s, 3H), 3.88 (s, 3H), 3.87 (s, 3H), 3.79 (s, 3H). ^{13}C NMR (101 MHz, $CDCl_3$) δ 198.45, 187.61, 163.15, 159.85, 148.55, 148.24, 146.76, 146.72, 146.41, 144.56, 138.37, 136.21, 131.77, 127.56, 126.97, 125.46, 123.87, 123.37, 120.34, 115.82, 114.79, 114.75, 110.36, 109.81, 105.15, 98.28, 56.05, 55.95, 55.53, 55.43.

(1*E*,6*E*)-4-(3-Fluorobenzylidene)-1,7-bis(4-hydroxy-3-methoxyphenyl)hepta-1,6-diene-3,5-dione (32). 3-Fluorobenzaldehyde (248 mg, 2 mmol) and **1** (368 mg, 1 mmol) were used as reactants, and column chromatography (petroleum ether/acetic ether 3:1) gave 329 mg of **32** as a yellow powder, yield 69%. HPLC t_R = 12.2 min; R_f = 0.32 (petroleum ether/acetic ether 1:1). HR-MS calcd for $C_{28}H_{23}O_6F_1$: 474.1473, found 474.1476. ^{1}H NMR (400 MHz, acetone) δ 7.90 (s, 1H), 7.69 (d, J = 15.5 Hz, 1H), 7.50 (d, J = 16.2 Hz, 1H), 7.39 (m, 2H), 7.39 (d, J = 15.5 Hz, 1H), 7.32 (d, J = 1.8 Hz, 1H), 7.31 (dd, J = 8.2, 1.8 Hz, 1H), 7.28 (dd, J = 8.4, 1.8 Hz, 1H), 7.12−7.17 (m, 1H), 7.11 (dd, J = 8.2, 1.8 Hz, 1H), 6.90 (d, J = 8.2 Hz, 1H), 6.85 (d, J = 16.2 Hz, 1H), 6.83 (d, J = 8.2 Hz, 1H), 3.90 (s, 3H), 3.88 (s, 3H). ^{13}C NMR (101 MHz, acetone) δ 197.59, 188.25, 163.48 (d, J = 244.6 Hz), 150.86, 150.62, 148.83, 148.77, 148.08, 145.78, 143.93, 138.30, 137.46 (d, J = 7.9 Hz), 131.54 (d, J = 8.4 Hz), 127.86, 127.33, 127.00 (d, J = 2.8 Hz), 125.68, 124.95, 124.35, 119.85, 117.47 (d, J = 21.4 Hz), 117.00 (d, J = 22.6 Hz), 116.31, 116.18, 112.43, 111.66, 56.42, 56.35.

(1*E*,6*E*)-4-(4-Fluorobenzylidene)-1,7-bis(4-hydroxy-3-methoxyphenyl)hepta-1,6-diene-3,5-dione (33). 4-Fluorobenzaldehyde (248 mg, 2 mmol) and **1** (368 mg, 1 mmol) were used as reactants, and column chromatography (petroleum ether/acetic ether 3:1) gave 311 mg of **33** as a yellow powder, yield 66%. HPLC t_R = 12.3 min; R_f = 0.31 (petroleum ether/acetic ether 1:1). HR-MS calcd for $C_{28}H_{23}O_6F_1$: 474.1473, found 474.1474. ^{1}H NMR (400 MHz, $CDCl_3$) δ 7.80 (s, 1H), 7.77 (d, J = 15.4 Hz, 1H), 7.50 (d, J = 8.5 Hz, 1H), 7.48 (d, J = 8.0 Hz, 1H), 7.45 (d, J = 16.2 Hz, 1H), 7.16 (dd, J = 8.2, 1.8 Hz, 1H), 7.04 (d, J = 2.0 Hz, 1H), 7.03 (dd, J = 8.2, 2.0 Hz, 1H), 7.03 (d, J = 8.2 Hz, 1H), 7.01 (d, J = 8.5 Hz, 1H), 6.97 (d, J = 1.8 Hz, 1H), 6.92 (d, J = 8.0 Hz, 1H), 6.93 (d, J = 15.4 Hz, 1H), 6.88 (d, J = 8.2 Hz, 1H), 6.77 (d, J = 16.2 Hz, 1H), 5.94 (s, 2H), 3.93 (s, 3H), 3.90 (s, 3H). ^{13}C NMR (101 MHz, acetone) δ 197.89, 188.22, 164.33 (d, J = 249.7 Hz), 150.76, 150.49, 148.78, 148.73, 147.77, 145.41, 142.61, 138.69, 133.26 (d, J = 8.7 Hz), 131.51 (d, J = 3.1 Hz), 127.89, 127.35, 125.74, 124.81, 124.23, 119.89, 116.58 (d, J = 21.9 Hz), 116.27, 116.15, 112.36, 111.63, 56.38, 56.31

(1*E*,6*E*)-4-(4-Ethylbenzylidene)-1,7-bis(4-hydroxy-3-methoxyphenyl)hepta-1,6-diene-3,5-dione (34). 4-Ethylbenzaldehyde (268 mg, 2 mmol) and **1** (368 mg, 1 mmol) were used as reactants, and column chromatography (petroleum ether/acetic ether 3:1) gave 288 mg of **34** as a yellow powder, yield 59%. HPLC t_R = 16.9 min; R_f = 0.36 (petroleum ether/acetic ether 1:1). HR-MS calcd for $C_{30}H_{28}O_6$: 484.1880, found 484.1881. ^{1}H NMR (400 MHz, $CDCl_3$) δ 7.83 (s, 1H), 7.75 (d, J = 15.4 Hz, 1H), 7.47 (d, J = 16.2 Hz, 1H), 7.42 (d, J = 8.2 Hz, 2H), 7.13−7.16 (m, 3H), 7.03 (d, J = 1.5 Hz, 1H), 7.01 (dd, J = 8.2, 1.6 Hz, 1H), 6.97 (d, J = 1.6 Hz,1H), 6.96 (d, J = 15.4 Hz, 1H), 6.91 (d, J = 8.2 Hz, 1H), 6.87 (d, J = 8.2 Hz, 1H), 6.80 (d, J = 16.2 Hz, 1H), 3.91 (s, 3H), 3.87 (s, 3H), 2.61 (q, J = 7.56 Hz, 2H), 1.19 (t, J = 7.59 Hz, 3H). ^{13}C NMR (101 MHz, $CDCl_3$) δ 198.43, 187.03, 148.84, 148.54, 147.51, 147.16, 146.82, 146.79, 145.39, 140.69, 139.77, 130.86, 130.61, 128.40, 127.28, 126.66, 125.38, 124.03, 123.67, 119.77, 114.86, 114.83, 110.36, 109.97, 56.06, 55.95, 28.75, 15.10.

(1*E*,6*E*)-4-(2,3-Dimethoxybenzylidene)-1,7-bis(4-hydroxy-3-methoxyphenyl)hepta-1,6-diene-3,5-dione (35). 2,3-Dimethoxybenzaldehyde (332 mg, 2 mmol) and **1** (368 mg, 1 mmol) were used as reactants, and column chromatography (petroleum ether/acetic ether 2:1) gave 180 mg of **35** as a yellow powder, yield 35%. HPLC t_R = 18.8 min; R_f = 0.24 (petroleum ether/acetic ether 1:1). HR-MS calcd for $C_{30}H_{28}O_8$ $[M - H]^-$: 515.1706, found 515.1696. ^{1}H NMR (400 MHz, $CDCl_3$) δ 8.13 (s, 1H), 7.75 (d, J = 15.5 Hz, 1H), 7.41 (d, J = 16.1 Hz, 1H), 7.16 (dd, J = 8.3, 1.5 Hz, 1H), 7.06 (d, J = 1.5 Hz, 1H), 6.98 (dd, J = 8.2, 1.5 Hz, 1H), 6.98 (d, J = 15.5 Hz, 1H), 6.97 (d, J = 1.5 Hz, 1H), 6.88−6.96 (m, 4H), 6.86 (d, J = 8.2 Hz, 1H), 6.70 (d, J = 16.1 Hz, 1H), 5.92 (s, 1H), 5.90 (s, 1H), 3.93 (s, 3H), 3.92 (s, 3H), 3.88 (s, 3H), 3.84 (s, 3H). ^{13}C NMR (101 MHz, $CDCl_3$) δ 197.56, 187.64, 152.67, 148.72, 148.54, 148.29, 147.05, 146.81, 145.46, 141.56, 136.00, 128.25, 127.30, 126.76, 125.45, 124.11, 123.95, 123.73, 121.82, 120.01, 114.86, 114.80, 114.35, 110.26, 109.81, 61.37, 56.04, 55.93, 55.83.

(1*E*,6*E*)-1,7-Bis(4-hydroxy-3-methoxyphenyl)-4-(3-methoxybenzylidene)hepta-1,6-diene-3,5-dione (36). 3-Methoxybenzaldehyde (272 mg, 2 mmol) and **1** (368 mg, 1 mmol) were used as reactants, and column chromatography (petroleum ether/acetic ether 2:1) gave 285 mg of **36** as a yellow powder, 59%. HPLC t_R = 11.6 min; R_f = 0.24 (petroleum ether/acetic ether 1:1). HR-MS calcd for $C_{29}H_{26}O_7$: 486.1679, found 486.1674. ^{1}H NMR (400 MHz, $CDCl_3$) δ 7.81 (s, 1H), 7.76 (d, J = 15.4 Hz, 1H), 7.45 (d, J = 16.1 Hz, 1H), 7.24 (dd, J = 8.0, 8.0 Hz, 1H), 7.16 (dd, J = 8.2, 1.9 Hz, 1H), 7.0−7.09 (m, 1H), 7.04 (d, J = 1.9 Hz, 1H), 7.02−7.03 (m, 1H), 7.02 (dd, J = 8.2, 1.9 Hz, 1H), 6.96 (d, J = 15.4 Hz, 1H), 6.95 (d, J = 1.9 Hz, 1H), 6.91 (d, J = 8.2 Hz, 1H), 6.87−6.89 (m, 1H), 6.87 (d, J = 8.2 Hz, 1H), 6.77 (d, J = 16.1 Hz, 1H), 5.97 (s, 2H), 3.92 (s, 3H), 3.88 (s, 3H), 3.76 (s, 3H). ^{13}C NMR (101 MHz, $CDCl_3$) δ 197.92, 187.01, 159.64, 148.86, 148.59, 147.51, 146.80, 146.77, 145.67, 141.09, 140.31, 134.86, 129.81, 127.25, 126.64, 125.28, 124.07, 123.77, 122.80, 119.74, 116.34, 115.15, 114.85, 114.83, 110.33, 109.90, 56.07, 55.96, 55.27.

(1*E*,6*E*)-1,7-Bis(3,4-dimethoxyphenyl)-4-((5-methylfuran-2-yl)methylene)hepta-1,6-diene-3,5-dione (37). 5-Methylfuran-2-carbaldehyde (220 mg, 2 mmol) and **3** (396 mg, 1 mmol) were used as reactants and the raw product was purified by column chromatography (petroleum ether/acetic ether 3:1) to give 276 mg of **37** as a yellow powder, yield 57%. HPLC t_R = 16.3 min; R_f = 0.32 (petroleum ether/acetic ether 1:1). HR-MS calcd for $C_{29}H_{28}O_7$: 488.1830, found 488.1828. ^{1}H NMR (500 MHz, $CDCl_3$) δ 7.74 (d, J = 15.4 Hz, 1H), 7.60 (s, 1H), 7.46 (d, J = 16.1 Hz, 1H), 7.17 (dd, J = 8.4, 1.9 Hz, 1H), 7.11 (dd, J = 8.4, 1.9 Hz, 1H), 7.05 (d, J = 1.9 Hz, 2H), 6.93 (d, J = 15.4 Hz, 1H), 6.90 (d, J = 16.1 Hz, 1H), 6.84 (d, J = 8.4 Hz, 2H), 6.72 (d, J = 3.4 Hz, 1H), 6.08 (dq, J = 3.4, 0.9 Hz, 1H), 3.89−3.90 (m, 12H), 2.26 (d, J = 0.9 Hz, 3H). ^{13}C NMR (101 MHz, $CDCl_3$) δ 197.53, 185.99, 157.42, 151.68, 151.55, 149.31, 149.22, 148.45, 146.25, 144.64, 134.83, 127.86, 127.39, 126.67, 126.25, 123.30, 123.25, 120.24, 120.16, 111.13, 110.60, 110.21, 109.74, 56.05, 56.03, 56.00, 55.95, 13.99.

General Procedures for Synthesis of 18 and 29. 3,4-Dimethoxybenzaldehyde (831 mg, 5 mmol) or 4-hydroxy-3-methoxybenzaldehyde (760 mg, 5 mmol) was mixed with pentane-2,4-dione (42 mg, 1 mmol) and 25 mL of toluene in a three-neck rounded flask equipped a water dispenser. Then pyridine (7.9 mg, 0.1 mmol, in 0.2 mL of toluene) and acetic acid (9.6 mg, 0.16 mmol, in 0.2 mL of toluene) were added in as catalysts. The reaction mixture was stirred at 140 °C overnight, and the generated water was removed by water dispenser during the whole reaction. After the mixture was washed with water to remove pyridine and acetic acid, the solvent was evaporated to get raw product. Finally the raw product was purified by column chromatography to give **18** and **29**, respectively.

(1*E*,6*E*)-4-(3,4-Dimethoxybenzylidene)-1,7-bis(3,4-dimethoxyphenyl)hepta-1,6-diene-3,5-dione (18). Column chromatography (petroleum ether/acetic ether 3:2) gave 381 mg of **18** as a yellow powder, yield 70%. HPLC t_R = 15.7 min; R_f = 0.28 (petroleum ether/acetic ether 1:1). ^{1}H NMR (500 MHz, $CDCl_3$) δ 7.80 (s, 1H), 7.75 (d, J = 15.4 Hz, 1H), 7.51 (d, J = 16.1 Hz, 1H), 7.18 (dd, J = 8.4, 2.0 Hz, 1H), 7.13 (dd, J = 8.4, 2.0 Hz, 1H), 7.05−7.06 (m, 3H), 6.98 (d, J = 2.0 Hz, 1H), 6.99 (d, J = 15.4 Hz, 1H), 6.85 (d, J = 8.4 Hz, 1H), 6.81 (d, J = 8.4 Hz, 2H), 6.81 (d, J = 16.1 Hz, 1H), 3.89 (s, 6H), 3.87 (s, 3H), 3.86 (s, 6H), 3.80 (s, 3H). ^{13}C NMR (101 MHz, $CDCl_3$) δ 198.39, 186.84, 152.01, 151.66, 151.21, 149.37, 149.30, 148.95, 146.90, 144.88, 140.65, 139.00,

127.86, 127.14, 126.39, 125.61, 124.98, 123.54, 123.27, 120.29, 112.99, 111.24, 111.19, 111.16, 110.75, 110.33, 56.05, 56.01, 55.94, 55.90, 55.87.

(1*E*,6*E*)-4-(4-Hydroxy-3-methoxybenzylidene)-1,7-bis(4-hydroxy-3-methoxyphenyl)hepta-1,6-diene-3,5-dione (29). Column chromatography (petroleum ether/acetic ether 2:3) gave 223 mg of **29** as a yellow powder, yield 44%. HPLC $t_R = 7.9$ min; $R_f =$ 0.39 (petroleum ether/acetic ether 1:2). HR-MS calcd for $C_{29}H_{26}O_8$: 502.1628, found 502.1623. ^{1}H NMR (400 MHz, $CDCl_3$) δ 7.80 (s, 1H), 7.75 (d, J = 15.4 Hz, 1H), 7.49 (d, J = 16.1 Hz, 1H), 7.16 (dd, J = 8.2, 1.7 Hz, 1H), 7.09 (dd, J = 8.3, 1.8 Hz, 1H), 7.04 (m, 2H), 7.03 (dd, J = 8.2, 1.8 Hz, 1H), 6.96 (d, J = 1.7 Hz, 1H), 6.95 (d, J = 15.4 Hz, 1H), 6.91 (d, J = 8.2 Hz, 1H), 6.88 (d, J = 8.2 Hz, 1H), 6.87 (d, J = 8.3 Hz, 1H), 6.80 (d, J = 16.1 Hz, 1H), 5.95 (s, 1H), 5.93 (s, 1H), 5.89 (s, 1H), 3.92 (s, 3H), 3.89 (s, 3H), 3.83 (s, 3H). ^{13}C NMR (101 MHz, acetone) δ 198.90, 188.17, 150.69, 150.37, 150.05, 148.84, 148.77, 148.37, 147.20, 144.77, 140.74, 140.11, 128.05, 127.48, 126.61, 126.13, 126.01, 124.64, 124.05, 120.15, 116.31, 116.25, 116.23, 114.39, 112.38, 111.75, 56.43, 56.35, 56.25.

General Procedures for the Synthesis of 38−40. Triethoxymethane (1.48 g, 10 mmol) and 1 mmol of corresponding symmetrical curcuminoids were dissolved in 5 mL of acetic anhydride. The reaction mixture was stirred at 140 °C for 5 h and then transferred to room temperature, and 10 mL of H_2O was added for an additional 10 min. The raw product was extracted by ethyl acetate and then purified by column chromatography or recrystallization.

4,4′-((1*E*,6*E*)-4-(Hydroxymethylene)-3,5-dioxohepta-1,6-diene-1,7-diyl)bis(2-methoxy-4,1-phenylene) Diacetate (38). 1 (368 mg, 1 mmol) was used as reactant and the raw product was purified by column chromatography (petroleum ether/acetic ether 4:1) to give 140 mg of **38** as a yellow powder, yield 29%. HPLC $t_R =$ 10.4 min; $R_f = 0.44$ (petroleum ether/acetic ether 3:2). HR-MS calcd for $C_{26}H_{24}O_9$: 480.1415, found 480.1409. ^{1}H NMR (400 MHz, $CDCl_3$) δ 10.35 (s, 1H), 7.93 (d, J = 15.5 Hz, 2H), 7.76 (d, J = 15.5 Hz, 2H), 7.27 (dd, J = 8.2, 1.6 Hz, 2H), 7.21 (d, J = 1.6 Hz, 2H), 7.10 (d, J = 8.2 Hz, 2H), 3.91 (s, 6H), 2.34 (s, 6H). ^{13}C NMR (400 MHz, $CDCl_3$) δ 189.36, 186.95, 168.67, 151.55, 145.09, 142.17, 133.63, 123.44, 122.18, 120.47, 112.77, 111.94, 56.03, 20.67.

(1*E*,6*E*)-4-(Hydroxymethylene)-1,7-bis(4-methoxyphenyl)-hepta-1,6-diene-3,5-dione (39). 2 (336 mg, 1 mmol) was used as reactant and the raw product was purified by column chromatography (petroleum ether/acetic ether 9:1) to give 255 mg of **39** as a yellow powder, yield 70%. HPLC $t_R = 9.9$ min; $R_f = 0.37$ (petroleum ether/acetic ether 3:1). HR-MS calcd for $C_{22}H_{20}O_5$: 364.1305, found 364.1292. ^{1}H NMR (400 MHz, $CDCl_3$) δ 10.35 (s, 1H), 7.94 (d, J = 15.4 Hz, 2H), 7.72 (d, J = 15.4 Hz, 2H), 7.61 (d, J = 8.2 Hz, 4H), 6.94 (d, J = 8.2 Hz, 4H), 3.87 (s, 6H). ^{13}C NMR (101 MHz, $CDCl_3$) δ 189.48, 187.14, 162.15, 145.44, 130.79, 127.60, 117.94, 114.54, 55.46.

(1*E*,6*E*)-1,7-Bis(3,4-dimethoxyphenyl)-4-(hydroxymethylene)-hepta-1,6-diene-3,5-dione (40). 3 (396 mg, 1 mmol) was used as reactant and the raw product was purified by recrystallization in acetic anhydride to give 273 mg of **40** as an orange powder, yield 64%. HPLC $t_R = 14.6$ min; $R_f = 0.40$ (petroleum ether/acetic ether 3:2). HR-MS calcd for $C_{24}H_{24}O_7$, 424.1517; found, 424.1518. ^{1}H NMR (400 MHz, $CDCl_3$) δ 10.37 (s, 1H), 7.93 (d, J = 15.4 Hz, 2H), 7.71 (d, J = 15.4 Hz, 2H), 7.26 (d, J = 8.1 Hz, 2H), 7.17 (s, 2H), 6.91 (d, J = 8.1 Hz, 2H), 3.97 (s, 6H), 3.95 (s, 6H). ^{13}C NMR (101 MHz, $CDCl_3$) δ 189.39, 187.23, 151.98, 149.35, 145.80, 127.83, 124.03, 118.04, 111.12, 110.26, 56.04, 56.01.

Biology. Cell Viability Assay. Sulforhodamine B (SRB) Method. Cells were maintained in RPMI with 5% fetal bovine serum (FBS) and penicillin/streptomycin in a 37 °C incubator with 5% CO_2. Cells were plated in 96-well plates and were treated with test agents on the following day and further incubated for 48 h before viability assay was carried out. The SRB assay was performed to evaluate cell viability with Thermo Scientific's Multiskan MK3 plate reader to obtain the GI_{50} values.

Alamar Blue Method. Cells were maintained in RPMI with 10% fetal bovine serum (FBS) and penicillin/streptomycin in a 37 °C incubator with 5% CO_2. Cells were plated in 384-well plates and were treated with test agents on the following day and further incubated for 72 h before the viability assay was carried out. The Alamar Blue assay was performed to evaluate cell viability with PerkinElmer's EnVision multimode plate reader to obtain the GI_{50} values.[42,43] The GI_{50} is defined as the concentration of agents that decreases viability by 50% in a total cell population compared to control cells with solvent vehicle at the end of the incubation period.

NF-κB Translocation Assay. In brief, A549 cell were seeded in 384-well plates, incubated for 15 h, then incubated with various concentrations of compounds for 30 min. TNF-α (10 ng/mL, final) was added to cells to stimulate the NF-κB cell signaling pathway for 30 min. Cells were then fixed with paraformaldehyde (2%, 100 μL) and permeabilized with Triton X-100 (0.1%, 100 μL). Finally, rabbit anti-p65 NF-κB antibody and goat anti-rabbit IgG with conjugated Alexa Fluor 488 were used to stain NF-κB, and Hoechst 33342 was used to stain nucleus. Fluorescence intensity of NF-κB and nuclear staining were recorded with an automated imaging system, ImageXpress5000A (Molecular Devices). The levels of NF-κB translocation were calculated and expressed as the difference between average fluorescence intensity in the nucleus and in the cytoplasm. After stimulation with TNF-α, the inhibitory effect of test compounds on TNFα induced NF-κB translocation was expressed as a percentage of fluorescence intensity difference (in nucleus and in cytoplasm) in the control wells (TNFα only) after subtracting background (no TNFα treatment). The IC_{50} of test compounds in this NF-κB translocation assay stands for the concentration of a compound required to induce 50% inhibition. All data are obtained as average values from triplicate samples, and the experiments were repeated at least three times.

Clonogenic Assay. A549 cells were plated in low density in a 12-well plate and treated with test compounds the following day and every 3 days thereafter. On day 9 after colonies were formed, cells were fixed with trichloroacetic acid (TCA) (10%) for 30 min at 4 °C, washed with water, stained with SRB, and then washed with acetic acid (1%). The images of the plate were scanned, and colonies were counted using image processing and analysis in Java (Image J, Research Service Branch, NIH).

IKK Assays. Cell Based IKK Assay. Cells were treated with various test agents for a defined period of time as described in each figure and were lysed for detection of phosphorylation status of IκB, a readout for IKK activity, and total IκB protein. The NP-40 lysates buffer was used (1.0% NP-40, 10 mM Hepes, pH 7.4, 150 mM NaCl, 5 mM NaF, 2 mM Na_3VO_4, 5 mM $Na_4P_2O_7$, 10 μg/mL aprotinin, 10 μg/mL leupeptin, 1 mM PMSF). For Western blotting, equal volumes of cell lysate were subject to electrophoresis on SDS−PAGE (12.5%). Proteins were then electrotransferred to a nitrocellulose membrane (GE Water and Process Technologies, Trevose, PA) as described previously.[44] Membranes were blocked in a solution of 5% nonfat dry milk in TBS-T buffer (20 mM Tris, pH 7.6, 500 mM NaCl, 0.5% Tween-20) for 30 min followed by incubation with anti-pS^{32}-I-κB or I-κB antibodies from Cell Signaling (Beverly, MA) for at least 2 h. The membrane was then washed and treated with the corresponding horseradish peroxidase conjugated anti-mouse immunoglobulin [Ig] or anti-rabbit Ig as indicated. Immunodetection was performed using West Pico (Pierce, Rockford, IL) or West Dura (Pierce) followed by imaging on Kodak's Image Station 2000R (New Haven, CT).

In Vitro IKK Assay. Activated recombinant IKKβ in MOPS buffer (8 mM MOPS-NaOH, pH 7.0, 200 μM EDTA, 15 mM $MgCl_2$) from Upstate Cell Signaling Solutions (Lake Placid, NY) was used for the in vitro kinase assay. The test compounds were incubated with IKKβ (40 ng) for 30 min at room temperature.

The addition of Mg-ATP mix (15 mM $MgCl_2$, 100 μM ATP, 8 mM MOPS-NaOH, pH 7.0, 5 mM β-glycerophosphate, 1 mM EGTA, 200 nM sodium orthovanadate, 200 nM DTT), purified GST- I-κBα (5 μg), and [γ-^{32}P]ATP (0.5 μCi) in a final volume of 25 μL started the reaction, which was allowed to proceed at 30 °C for 30 min. Reactions were terminated by boiling the kinase reaction solution in a 6× SDS sample buffer for 5 min. The samples were resolved on SDS−PAGE (12.5%). The gel was stained with Coomassie Blue dye (0.05%). ^{32}P incorporation into GST-I-κBα was assessed by autoradiography. In addition, the radiolabeled GST-I-κBα protein bands were excised for quantification with a scintillation counter (Beckman LS 6500, Beckman Coulter, Fullerton, CA).

Molecular Modeling. Homology Model Building. IKKβ catalytic domain sequence (code O14920) was collected from UniProt (http://www.uniprot.org/), and C terminal amino acid residues after G218, which are difficult to be modeled, were deleted since it is far away from ATP binding pocket. The sequence similarity search of IKKβ catalytic domain was performed using the BLAST protocol which is built in Discovery Studio 2.1 (Accelrys Inc.). Four templates 2JC6, 1A06, 2QNJ, and 2A2A were chosen from Protein Data Bank (PDB). The C terminal amino acids after a conserved glycine were deleted from all the templates. The automated sequence alignment and analysis of template and target were carried out by Discovery Studio 2.1.

The homology modeling of the IKKβ catalytic domain was carried out by using the built-in Modeler package of Discovery Studio 2.1. The four different kinase templates sequences were aligned together with the IKKβ sequence, and this alignment was supplied along with the 3D coordinates of templates as an input to the program. The best model given by the program was chosen, and energy minimization was done by using the Powell method for about 1000 iterations, with Tripos force field in Sybyl 7.3.5. The structural analysis was carried out with the Ramanchandran plot in Sybyl 7.3.5.

Small Molecular Preparation. The 3D structure of ATP was extracted from the crystal structures of the phosphorylase kinase (PDB code 1PHK, 28.6% sequence identity with IKKβ catalytic domain). The geometries of compound **17** were energy minimized using density functional theory. These calculations were performed with the B3LYP hybrid functional and the 6-31G basis set implemented in Gaussian 03, revision E.01, software package.[45] After energy minimization, it adopts a propeller-shaped conformation.

Docking. Molecular docking studies of compounds with the ATP binding pocket were performed with Surflex-Dock in Sybyl 7.3.5. Automatic was chosen as the mode of construction for the protomol. Threshold is 0.5 and bloat is 0.

Acknowledgment. We thank Mary Puckett for critical reading of the manuscript. This work was supported in part by grants from the MOST of China (863 Program 2008AA02Z304) and NSFC (Grant 30973619) (X.B.) and from the U.S. National Institutes of Health (Grant P01 CA116676 to H.F.) and Emory Faculty Distinction Fund (H.F.). H.F. is a GCC Distinguished Cancer Scholar and a GRA Distinguished Investigator. Y.D. is a recipient of Emory Head and Neck Cancer SPORE Career Development Award (Grant P50 CA128613).

Supporting Information Available: ^{1}H NMR, ^{13}C NMR, HRMS, and HPLC spectra; additional cancer cell growth inhibition data and molecular modeling information. This material is available free of charge via the Internet at http://pubs.acs.org.

References

(1) Ghosh, S.; May, M.; Kopp, E. NF-κB and Rel proteins: evolutionarily conserved mediators of immune responses. *Annu. Rev. Immunol.* **1998**, *16*, 225–260.
(2) Hayden, M.; Ghosh, S. Shared principles in NF-κB signaling. *Cell* **2008**, *132*, 344–362.
(3) Bonizzi, G.; Karin, M. The two NF-κB activation pathways and their role in innate and adaptive immunity. *Trends Immunol.* **2004**, *25*, 280–288.
(4) Shukla, S.; MacLennan, G.; Fu, P.; Patel, J.; Marengo, S.; Resnick, M.; Gupta, S. Nuclear factor-nB/p65 (Rel A) is constitutively activated in human prostate adenocarcinoma and correlates with disease progression. *Neoplasia* **2004**, *6*, 390–400.
(5) Ni, H.; Ergin, M.; Huang, Q.; Qin, J.; Amin, H.; Martinez, R.; Saeed, S.; Barton, K.; Alkan, S. Analysis of expression of nuclear factor κB (NF-κB) in multiple myeloma: downregulation of NF-κB induces apoptosis. *Br. J. Haematol.* **2001**, *115*, 279–286.
(6) Guzman, M.; Neering, S.; Upchurch, D.; Grimes, B.; Howard, D.; Rizzieri, D.; Luger, S.; Jordan, C. Nuclear factor-κB is constitutively activated in primitive human acute myelogenous leukemia cells. *Blood* **2001**, *98*, 2301–2037.
(7) Tang, X.; Shishodia, S.; Behrens, C.; Hong, W.; Wistuba, I. Nuclear factor-κB (NF-κB) is frequently expressed in lung cancer and preneoplastic lesions. *Cancer* **2006**, *107*, 2637–2646.
(8) Huang, S.; DeGuzman, A.; Bucana, C.; Fidler, I. Nuclear factor-κB activity correlates with growth, angiogenesis, and metastasis of human melanoma cells in nude mice. *Clin. Cancer Res.* **2000**, *6*, 2573–2581.
(9) Farina, A.; Tacconelli, A.; Vacca, A.; Maroder, M.; Gulino, A.; Mackay, A. Transcriptional up-regulation of matrix metalloproteinase-9 expression during spontaneous epithelial to neuroblast phenotype conversion by SK-N-SH neuroblastoma cells, involved in enhanced invasivity, depends upon GT-Box and nuclear factor κB elements. *Cell Growth Differ.* **1999**, *10*, 353–367.
(10) Wang, C.; Mayo, M.; Korneluk, R.; Goeddel, D.; Baldwin, A., Jr. NF-B antiapoptosis: induction of TRAF1 and TRAF2 and c-IAP1 and c-IAP2 to suppress caspase-8 activation. *Science* **1998**, *281*, 1680–1683.
(11) Karin, M. Nuclear factor-κB in cancer development and progression. *Nature* **2006**, *441*, 431–436.
(12) Qiao, L.; Zhang, H.; Yu, J.; Francisco, R.; Dent, P.; Ebert, M.; Rocken, C.; Farrell, G. Constitutive activation of NF-κB in human hepatocellular carcinoma: evidence of a cytoprotective role. *Hum. Gene Ther.* **2006**, *17*, 280–290.
(13) Arlt, A.; Gehrz, A.; Müerköster, S.; Vorndamm, J.; Kruse, M.-L.; Fölsch, U. R.; Schäfer, H. Role of NF-κB and Akt/PI3K in the resistance of pancreatic carcinoma cell lines against gemcitabine-induced cell death. *Oncogene* **2003**, *22*, 3243–3251.
(14) Gradilone, A.; Silvestri, I.; Scarpa, S.; Morrone, S.; Gandini, O.; Pulcinelli, F.; Gianni, W.; Frati, L.; Agliano, A.; Gazzaniga, P. Failure of apoptosis and activation on NFκB by celecoxib and aspirin in lung cancer cell lines. *Oncol. Rep.* **2007**, *17*, 823–828.
(15) Notarbartolo, M.; Poma, P.; Perri, D.; Dusonchet, L.; Cervello, M.; D'Alessandro, N. Antitumor effects of curcumin, alone or in combination with cisplatin or doxorubicin, on human hepatic cancer cells. Analysis of their possible relationship to changes in NF-κB activation levels and in IAP gene expression. *Cancer Lett.* **2005**, *224*, 53–65.
(16) Wang, X.; Ju, W.; Renouard, J.; Aden, J.; Minsky, S. A.; Lin, Y. 17-Allylamino-17-demethoxygeldanamycin synergistically potentiates tumor necrosis factor-induced lung cancer cell death by blocking the nuclear factor-κB pathway. *Cancer Res.* **2006**, *66*, 1089–1095.
(17) Sarkar, F.; Li, Y. Soy isoflavones and cancer prevention. *Cancer Invest.* **2003**, *21*, 744–757.
(18) Holmes-McNary, M.; Baldwin, A., Jr. Chemopreventive properties of trans-resveratrol are associated with inhibition of activation of the IκB kinase. *Cancer Res.* **2000**, *60*, 3477–3483.
(19) Plummer, S.; Holloway, K.; Manson, M.; Munks, R.; Kaptein, A.; Farrow, S.; Howells, L. Inhibition of cyclo-oxygenase 2 expression in colon cells by the chemopreventive agent curcumin involves inhibition of NF-κB activation via the NIK/IKK signalling complex. *Oncogene* **1999**, *18*, 6013–6020.
(20) Maheshwari, R.; Singh, A.; Gaddipati, J.; Srimal, R. Multiple biological activities of curcumin: a short review. *Life Sci.* **2006**, *78*, 2081–2087.
(21) Cheng, A.; Hsu, C.; Lin, J.; Hsu, M.; Ho, Y.; Shen, T.; Ko, J.; Lin, J.; Lin, B.; Ming-Shiang, W. Phase I clinical trial of curcumin, a chemopreventive agent, in patients with high-risk or pre-malignant lesions. *Anticancer Res.* **2001**, *21*, 2895–2900.
(22) Singh, S.; Aggarwal, B. Activation of transcription factor NF-κB is suppressed by curcumin (diferuloylmethane). *J. Biol. Chem.* **1995**, *270*, 24995–25000.
(23) Leu, T.; Maa, M. The molecular mechanisms for the antitumorigenic effect of curcumin. *Curr. Med. Chem.: Anti-Cancer Agents* **2002**, *2*, 357–370.
(24) Milacic, V.; Banerjee, S.; Landis-Piwowar, K.; Sarkar, F.; Majumdar, A.; Dou, Q. Curcumin inhibits the proteasome activity in human

colon cancer cells in vitro and in vivo. *Cancer Res*. **2008**, *68*, 7283–7292.
(25) Anand, P.; Kunnumakkara, A.; Newman, R.; Aggarwal, B. Bioavailability of curcumin: problems and promises. *Mol. Pharmaceutics* **2007**, *4*, 807–818.
(26) Ohtsu, H.; Xiao, Z.; Ishida, J.; Nagai, M.; Wang, H.; Itokawa, H.; Su, C.; Shih, C.; Chiang, T.; Chang, E. Antitumor agents. 217. Curcumin analogues as novel androgen receptor antagonists with potential as anti-prostate cancer agents. *J. Med. Chem*. **2002**, *45*, 5037–5042.
(27) Lin, L.; Shi, Q.; Nyarko, A.; Bastow, K.; Wu, C.; Su, C.; Shih, C.; Lee, K. Antitumor agents. 250. Design and synthesis of new curcumin analogs as potential anti-prostate cancer agents. *J. Med. Chem*. **2006**, *49*, 3963–3972.
(28) Zambre, A.; Kulkarni, V.; Padhye, S.; Sandur, S.; Aggarwal, B. Novel curcumin analogs and proliferation targeting TNF-induced NF-kappa B activation in human leukemic KBM-5 cells. *Bioorg. Med. Chem*. **2006**, *14*, 7196–7204.
(29) Weber, W.; Hunsaker, L.; Roybal, C.; Bobrovnikova-Marjon, E.; Abcouwer, S.; Royer, R.; Deck, L.; Vander Jagt, D. Activation of NFκB is inhibited by curcumin and related enones. *Bioorg. Med. Chem*. **2006**, *14*, 2450–2461.
(30) Adams, B.; Ferstl, E.; Davis, M.; Herold, M.; Kurtkaya, S.; Camalier, R.; Hollingshead, M.; Kaur, G.; Sausville, E.; Rickles, F. Synthesis and biological evaluation of novel curcumin analogs as anti-cancer and anti-angiogenesis agents. *Bioorg. Med. Chem*. **2004**, *12*, 3871–3883.
(31) Padhye, S.; Chavan, D.; Pandey, S.; Deshpande, J.; Swamy, K. V.; Sarkar, F. H. Perspectives on chemopreventive and therapeutic potential of curcumin analogs in medicinal chemistry. *Mini-Rev. Med. Chem*. **2010**, *10*, 372–387.
(32) Padhye, S.; Yang, H.; Jamadar, A.; Cui, Q.; Chavan, D.; Dominiak, K.; McKinney, J.; Banerjee, S.; Dou, Q.; Sarkar, F. New difluoro Knoevenagel condensates of curcumin, their schiff bases and copper complexes as proteasome inhibitors and apoptosis inducers in cancer cells. *Pharm. Res*. **2009**, 1–7.
(33) Padhye, S.; Banerjee, S.; Chavan, D.; Pandye, S.; Swamy, K. V.; Ali, S.; Li, J.; Dou, Q. P.; Sarkar, F. H. Fluorocurcumins as cyclooxygenase-2 inhibitor: molecular docking, pharmacokinetics and tissue distribution in mice. *Pharm. Res*. **2009**, *26*, 2438–2445.
(34) Ohtsu, H.; Xiao, Z.; Ishida, J.; Nagai, M.; Wang, H. K.; Itokawa, H.; Su, C. Y.; Shih, C.; Chiang, T.; Chang, E.; Lee, Y.; Tsai, M. Y.; Chang, C.; Lee, K. H. Antitumor agents. 217. Curcumin analogues as novel androgen receptor antagonists with potential as anti-prostate cancer agents. *J. Med. Chem*. **2002**, *45*, 5037–5042.
(35) Qiu, X.; Liu, Z.; Shao, W. Y.; Liu, X.; Jing, D. P.; Yu, Y. J.; An, L. K.; Huang, S. L.; Bu, X. Z.; Huang, Z. S.; Gu, L. Q. Synthesis and evaluation of curcumin analogues as potential thioredoxin reductase inhibitors. *Bioorg. Med. Chem*. **2008**, *16*, 8035–8041.
(36) Adams, B. K.; Ferstl, E. M.; Davis, M. C.; Herold, M.; Kurtkaya, S.; Camalier, R. F.; Hollingshead, M. G.; Kaur, G.; Sausville, E. A.; Rickles, F. R.; Snyder, J. P.; Liotta, D. C.; Shoji, M. Synthesis and biological evaluation of novel curcumin analogs as anti-cancer and anti-angiogenesis agents. *Bioorg. Med. Chem*. **2004**, *12*, 3871–3883.
(37) Kasinski, A.; Du, Y.; Thomas, S.; Zhao, J.; Sun, S.; Khuri, F.; Wang, C.; Shoji, M.; Sun, A.; Snyder, J. Inhibition of IκB kinase-nuclear factor-κB signaling pathway by 3,5-bis(2-flurobenzylidene)piperidin-4-one (EF24), a novel monoketone analog of curcumin. *Mol. Pharmacol*. **2008**, *74*, 654.
(38) Aggarwal, S.; Ichikawa, H.; Takada, Y.; Sandur, S. K.; Shishodia, S.; Aggarwal, B. B. Curcumin (diferuloylmethane) down-regulates expression of cell proliferation and antiapoptotic and metastatic gene products through suppression of IκBα kinase and Akt activation. *Mol. Pharmacol*. **2006**, *69*, 195–206.
(39) Baud, V.; Karin, M. Signal transduction by tumor necrosis factor and its relatives. *Trends Cell Biol*. **2001**, *11*, 372–377.
(40) Silverman, N.; Maniatis, T. NF-κB signaling pathways in mammalian and insect innate immunity. *Genes Dev*. **2001**, *15*, 2321–2342.
(41) Shoemaker, R.; Wolpert-DeFilippes, M.; Kern, D.; Lieber, M.; Makuch, R.; Melnick, N.; Miller, W.; Salmon, S.; Simon, R.; Venditti, J. Application of a human tumor colony-forming assay to new drug screening. *Cancer Res*. **1985**, *45*, 2145–2153.
(42) Rubinstein, L. V.; Shoemaker, R. H.; Paull, K. D.; Simon, R. M.; Tosini, S.; Skehan, P.; Scudiero, D. A.; Monks, A.; Boyd, M. R. Comparison of in vitro anticancer-drug-screening data generated with a tetrazolium assay versus a protein assay against a diverse panel of human tumor cell lines. *J. Natl. Cancer Inst*. **1990**, *82*, 1113–1118.
(43) Skehan, P.; Storeng, R.; Scudiero, D.; Monks, A.; McMahon, J.; Vistica, D.; Warren, J. T.; Bokesch, H.; Kenney, S.; Boyd, M. R. New colorimetric cytotoxicity assay for anticancer-drug screening. *J. Natl. Cancer Inst*. **1990**, *82*, 1107–1112.
(44) Zhang, L.; Chen, J.; Fu, H. Suppression of apoptosis signal-regulating kinase 1-induced cell death by 14-3-3 proteins. *Proc. Natl. Acad. Sci. U.S.A*. **1999**, *96*, 8511–8515.
(45) Frisch, M. J.; Trucks, G. W.; Schlegel, H. B.; Scuseria, G. E.; Robb, M. A.; Cheeseman, J. R.; Montgomery, J. A.; , Jr., Vreven, T.; Kudin, K. N.; Burant, J. C.; Millam, J. M.; Iyengar, S. S.; Tomasi, J.; Barone, V.; Mennucci, B.; Cossi, M.; Scalmani, G.; Rega, N.; Petersson, G. A.; Nakatsuji, H.; Hada, M.; Ehara, M.; Toyota, K.; Fukuda, R.; Hasegawa, J.; Ishida, M.; Nakajima, T.; Honda, Y.; Kitao, O.; Nakai, H.; Klene, M.; Li, X.; Knox, J. E.; Hratchian, H. P.; Cross, J. B.; Bakken, V.; Adamo, C.; Jaramillo, J.; Gomperts, R.; Stratmann, R. E.; Yazyev, O.; Austin, A. J.; Cammi, R.; Pomelli, C.; Ochterski, J. W.; Ayala, P. Y.; Morokuma, K.; Voth, G. A.; Salvador, P.; Dannenberg, J. J.; Zakrzewski, V. G.; Dapprich, S.; Daniels, A. D.; Strain, M. C.; Farkas, O.; Malick, D. K.; Rabuck, A. D.; Raghavachari, K.; Foresman, J. B.; Ortiz, J. V.; Cui, Q.; Baboul, A. G.; Clifford, S.; Cioslowski, J.; Stefanov, B. B.; Liu, G.; Liashenko, A.; Piskorz, P.; Komaromi, I.; Martin, R. L.; Fox, D. J.; Keith, T.; Al-Laham, M. A.; Peng, C. Y.; Nanayakkara, A.; Challacombe, M.; Gill, P. M. W.; Johnson, B.; Chen, W.; Wong, M. W.; Gonzalez, C.; Pople, J. A. *Gaussian 03*, revision E.01; Gaussian, Inc.: Wallingford, CT, 2004.